The VLDL receptor promotes lipotoxicity and increases mortality in mice following an acute myocardial infarction

Jeanna C. Perman,[1,2] Pontus Boström,[1,2] Malin Lindbom,[1,2] Ulf Lidberg,[1,2] Marcus StÅhlman,[1,2] Daniel Hägg,[1,2] Henrik Lindskog,[1,2] Margareta Scharin Täng,[1,2] Elmir Omerovic,[1,2] Lillemor Mattsson Hultén,[1,2] Anders Jeppsson,[2] Petur Petursson,[2] Johan Herlitz,[2] Gunilla Olivecrona,[3] Dudley K. Strickland,[4] Kim Ekroos,[5] Sven-Olof Olofsson,[1,2] and Jan Borén[1,2]

[1]Sahlgrenska Center for Cardiovascular and Metabolic Research, Wallenberg Laboratory, Sahlgrenska University Hospital, Göteborg, Sweden. [2]Institute of Medicine, Department of Molecular and Clinical Medicine, Sahlgrenska Academy at University of Gothenburg, Göteborg, Sweden. [3]Department of Medical Biosciences/Physiological Chemistry, UmeÅ University, UmeÅ, Sweden. [4]Center for Vascular and Inflammatory Disease, University of Maryland School of Medicine, Baltimore, Maryland, USA. [5]Zora Biosciences, Espoo, Finland.

Impaired cardiac function is associated with myocardial triglyceride accumulation, but it is not clear how the lipids accumulate or whether this accumulation is detrimental. Here we show that hypoxia/ischemia-induced accumulation of lipids in HL-1 cardiomyocytes and mouse hearts is dependent on expression of the VLDL receptor (VLDLR). Hypoxia-induced VLDLR expression in HL-1 cells was dependent on HIF-1α through its interaction with a hypoxia-responsive element in the *Vldlr* promoter, and VLDLR promoted the endocytosis of lipoproteins. Furthermore, *VLDLR* expression was higher in ischemic compared with nonischemic left ventricles from human hearts and was correlated with the total lipid droplet area in the cardiomyocytes. Importantly, *Vldlr*$^{-/-}$ mice showed improved survival and decreased infarct area following an induced myocardial infarction. ER stress, which leads to apoptosis, is known to be involved in ischemic heart disease. We found that ischemia-induced ER stress and apoptosis in mouse hearts were reduced in *Vldlr*$^{-/-}$ mice and in mice treated with antibodies specific for VLDLR. These findings suggest that VLDLR-induced lipid accumulation in the ischemic heart worsens survival by increasing ER stress and apoptosis.

Introduction

Reduced oxygen availability promotes triglyceride accumulation in hearts (1) and cardiomyocytes (2). Although it is well established that lipid accumulation in hypoxic conditions can be at least partly explained by a metabolic shift from oxidation of glucose and fatty acids to glycolysis (3, 4), it is not clear whether these metabolic changes alone are sufficient or if there is also a requirement for increased uptake of lipids. Potential mechanisms for lipid uptake include receptor-mediated endocytosis of lipoproteins, lipoprotein lipase–catalyzed (LPL-catalyzed) hydrolysis of triglycerides (5), and protein-facilitated uptake of fatty acids (reviewed in ref. 6).

Accumulation of triglycerides in the myocardium is associated with impaired cardiac function (7–10), but it is not known whether there is a causative link between these 2 phenomena. Intracellular triglycerides, which are stored in the hydrophobic core of lipid droplets and surrounded by amphipathic lipids and proteins (reviewed in ref. 11), are most likely very inert and thus not directly lipotoxic (12). However, it is possible that products formed during the degradation of triglycerides, such as diglycerides and fatty acids, and ceramides, which are formed from fatty acids, may have a pronounced effect on myocardial function and survival.

Hypoxia/ischemia is also known to promote ER stress or the unfolded protein response. This response involves the production of chaperones to promote the folding process and maintain ER homeostasis, but unresolved ER stress leads to apoptotic cell death (reviewed in refs. 13, 14). Recent evidence suggests that ER stress plays an important role in the progression of cardiovascular diseases including ischemic heart disease, indicating that strategies to reduce ER stress may be beneficial in the ischemic heart (15).

The aims of this investigation were to clarify the mechanisms behind the accumulation of lipids in the myocardium during ischemia and to determine the effect of lipid accumulation on survival following an acute myocardial infarction. We show that hypoxia/ischemia increased expression of the VLDL receptor (VLDLR) in HL-1 cardiomyocytes and mouse hearts, and that expression of the VLDLR was essential for lipid accumulation during hypoxia/ischemia. Furthermore, *VLDLR* mRNA expression was higher in ischemic versus nonischemic human hearts. Importantly, survival was increased and infarct size, ER stress, and apoptosis were reduced in *Vldlr*$^{-/-}$ compared with *Vldlr*$^{+/+}$ mice following an induced myocardial infarction. We also demonstrated that blockade of the VLDLR with antibodies reduced ischemia-induced lipid accumulation, ER stress, and apoptosis in mouse heart tissue. We therefore propose that the VLDLR-induced lipid accumulation in the ischemic heart worsens survival by increasing ER stress and apoptosis.

Results

Lipid droplets accumulate in ischemic mouse heart tissue and hypoxic HL-1 cells. An experimentally induced myocardial infarction in mice resulted in increases in the area of Oil Red O–stained lipid droplets and triglyceride content in heart tissue (Figure 1A), in agreement with previous studies in dogs (1). Hypoxic treatment of HL-1 cardiomyocytes also promoted an accumulation of Oil Red O–stained lipid droplets

Authorship note: Sven-Olof Olofsson and Jan Borén contributed equally to this work.

Conflict of interest: The authors have declared that no conflict of interest exists.

Citation for this article: *J Clin Invest.* 2011;121(7):2625–2640. doi:10.1172/JCI43068.

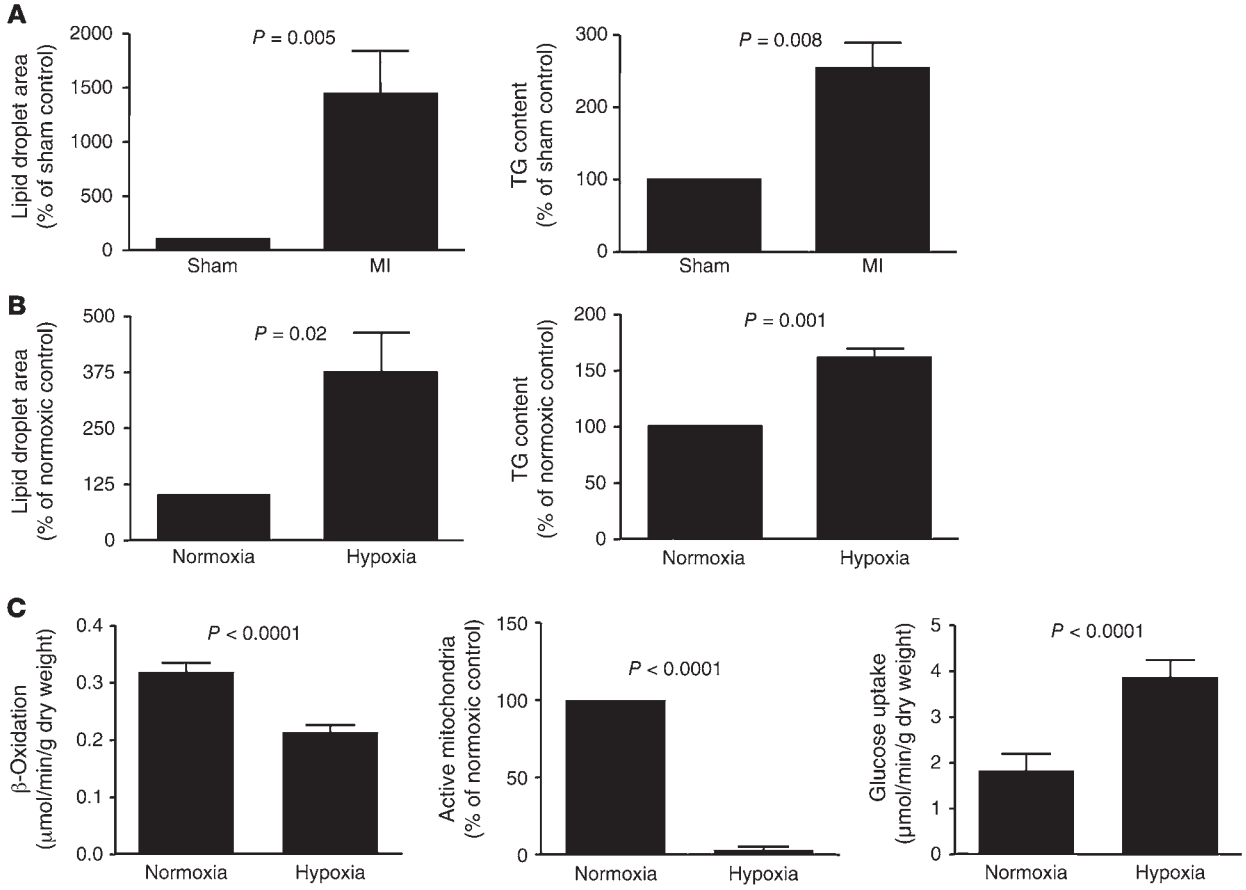

Figure 1

Ischemia/hypoxia induces triglyceride (TG) accumulation in mouse hearts and HL-1 cells, and decreases β-oxidation and increases glucose uptake in HL-1 cells. (**A**) The total area of Oil Red O–stained lipid droplets (left) and triglyceride content (right) in hearts from mice 6 hours after a sham operation or an experimentally induced myocardial infarction (MI) (n = 11–13). (**B**) The total area of Oil Red O–stained lipid droplets (left) and triglyceride content (right) in HL-1 cells incubated in normoxia or hypoxia for 8 hours (n = 6). (**C**) β-Oxidation, active mitochondria, and glucose uptake in HL-1 cells incubated in normoxia or hypoxia for 8 hours (n = 3). Results are shown as mean ± SEM.

and triglycerides (Figure 1B). In contrast, hypoxic treatment did not affect the levels of cholesterol, cholesterol ester, or phosphatidylcholine in HL-1 cells (Supplemental Table 1; supplemental material available online with this article; doi:10.1172/JCI43068DS1).

The uptake of radiolabeled oleic acid was significantly higher in cells incubated in hypoxia compared with normoxia (Supplemental Figure 1), indicating that hypoxia promotes increased uptake of fatty acids. We therefore investigated whether hypoxia increases the expression of proteins involved in the uptake of fatty acids. Hypoxic treatment of HL-1 cells reduced the mRNA expression of fatty acid binding protein (FABP) and did not affect the mRNA expression of fatty acid transport protein (FATP) or CD36 (Supplemental Figure 2A). Furthermore, hypoxia did not significantly affect the protein levels of FABP or FATP (Supplemental Figure 2B). It has been reported that hypoxia increases fatty acid transport in the heart by promoting a shift of CD36 from the interior of the cells to the plasma membrane (16). However, we did not observe increased surface expression of CD36 on hypoxic HL-1 cells (Supplemental Figure 2C). These results indicate that the increased accumulation of lipids in the HL-1 cells during hypoxia is not due to an increased expression of proteins involved in the uptake of fatty acids.

We observed decreased β-oxidation, a reduced level of oxidative active mitochondria, and increased glucose uptake in hypoxic HL-1 cells (Figure 1C). The decrease in mitochondrial β-oxidation may influence the amount of cellular fatty acids available for triglyceride biosynthesis. Thus, it is likely that the hypoxia-induced accumulation of triglycerides in HL-1 cells is at least partially explained by a metabolic shift away from oxidation of fatty acids toward glycolysis.

VLDLR expression is increased in hypoxic HL-1 cells and ischemic mouse heart tissue. To gain further insight into the key factors that play a role in hypoxia-induced lipid accumulation, we performed an Affymetrix gene array of normoxic and hypoxic HL-1 cardiomyocytes (a subset is shown in Table 1; full analysis can be viewed online, at http://www.ncbi.nlm.nih.gov/gds?term=GSE27975) and confirmed hypoxia-induced changes in gene expression by RT-PCR (Table 1). To determine whether similar changes occurred in ischemic heart tissue, we also used RT-PCR to analyze heart tissue from mice after a sham operation or an experimentally induced myocardial infarction (Table 1).

We observed changes in response to hypoxia in the expression of genes involved in fatty acid and glucose metabolism and in glucose transport in HL-1 cells, and these changes were consistent with a shift away from β-oxidation and toward glycolysis (Table 1).

Table 1
Hypoxia/ischemia-induced changes in gene expression in HL-1 cells and mouse hearts

Function			HL-1 cells		Heart tissue	
Gene title (Affymetrix probe set number)	**Gene symbol**	**Array FC**	**RT-PCR FC**	***P* value**	**RT-PCR FC**	***P* value**
Fatty acid and glucose metabolism						
Acyl-CoA synthetase long-chain family member 1 (1450643_at)	*Acsl1*	0.6	0.34 ± 0.03	0.02	ND	ND
Carnitine palmitoyltransferase 1a, liver (1460409_at)	*Cpt1a*	0.6	0.60 ± 0.01	0.03	0.64 ± 0.42	0.08
Carnitine palmitoyltransferase 1b, muscle (1418328_at)	*Cpt1b*	0.7	1.00 ± 0.30	NS	0.64 ± 0.33	0.03
Fatty acid synthase (1423828_at)	*Fasn*	0.6	ND	ND	ND	ND
Lactate dehydrogenase 1, A chain (1419737_a_at)	*Ldha*	1.7	2.00 ± 0.06	0.0001	ND	ND
Phosphofructokinase 1 (1439148_a_at)	*Pfk1*	3.5	3.43 ± 0.11	0.005	1.62 ± 0.55	0.04
Pyruvate dehydrogenase kinase, isoenzyme 1 (1423747_a_at)	*Pdk1*	5.1	4.81 ± 0.58	<0.001	ND	ND
Glucose transport						
Solute carrier family 2 (facilitated glucose transporter), member 1 (1426599_a_at)	*Slc2a1*	5.1	6.16 ± 0.02	<0.0001	ND	ND
Lipid storage and uptake						
Very low density lipoprotein receptor (1417900_at)	*Vldlr*	4.3	3.50 ± 0.23	<0.0001	1.70 ± 0.57	0.02

DNA microarray was performed on HL-1 cells, and hypoxia-induced changes in gene expression were confirmed by RT-PCR ($n = 9$). RT-PCR was also performed on heart tissue from sham-operated mice and mice with experimentally induced myocardial infarction to induce ischemia ($n = 5$). Data are expressed as fold change (FC) ± SEM between hypoxia/ischemia and normoxia/sham. ND, not determined.

In addition, and of particular interest, we found increases in *Vldlr* gene expression in both hypoxic HL-1 cells and ischemic heart tissue that were shown by RT-PCR analysis to be highly significant (Table 1). Immunoblot analysis demonstrated that VLDLR protein expression was 1.96- ± 0.14-fold higher ($P = 0.005$; $n = 6$) in hypoxic HL-1 cells and 2.41- ± 0.28-fold higher ($P = 0.002$; $n = 6$) in ischemic heart tissue. In addition, higher levels of VLDLR in hypoxic HL-1 cells were verified by immunohistochemistry (Supplemental Figure 3).

The VLDLR is essential for hypoxia/ischemia-induced lipid accumulation. We investigated whether the increased VLDLR expression observed in response to hypoxia/ischemia might play a role in promoting lipid accumulation. Knockdown of VLDLR by siRNA (Supplemental Figure 4, A and B) reduced the lipid droplet area in normoxic HL-1 cells and abolished the hypoxia-induced accumulation of lipid droplets (Figure 2A and Supplemental Figure 4C) and increase in triglyceride content (Figure 2A). In addition, we showed that the increases in lipid droplet area and triglyceride content in heart tissue from mice after an experimentally induced myocardial infarction were abolished in *Vldlr*$^{-/-}$ mice (Figure 2B). Our data thus show that the VLDLR is essential for lipid accumulation in response to oxygen deficiency both in vitro and in vivo.

Increased VLDLR expression is dependent on HIF-1α. Increased VLDLR expression appears to be a general response to lack of oxygen, as we demonstrated hypoxia-induced increases in VLDLR expression in a number of different cell types (Supplemental Table 2). We therefore investigated whether the hypoxia-induced expression of VLDLR was dependent on the transcription factor HIF-1α, which has been described as being involved in regulation of cardiac peptides under conditions of low oxygen (17). As expected, HIF-1α expression was increased in hypoxic cells (Figure 3A). Transfection of HL-1 cells with HIF-1α siRNA reduced the hypoxia-induced increase in VLDLR expression (Figure 3A and Supplemental Figure 5). In addition, stabilization of HIF-1α by dimethyloxalylglycine (DMOG) resulted in significantly increased expression of VLDLR (Figure 3B). Furthermore, DMOG promoted a large increase in the accumulation of lipid droplets in HL-1 cells, which was reversed by VLDLR knockdown (Figure 3C). Together these findings indicate that the hypoxia-induced increase in VLDLR expression is dependent on HIF-1α.

Identification of a hypoxia-responsive element in the promoter region of the Vldlr gene. To identify the molecular mechanism behind the effect of hypoxia on the expression of the VLDLR, we performed receptor gene assays using truncations of the VLDLR promoter coupled to the luciferase gene and measured the luciferase activity relative to the transfection control (*Renilla* luciferase) at normoxia and hypoxia. We observed a hypoxia-induced increase in the relative luciferase activity of the construct pGL3*Vldlr*180 (–180 bp to ATG) that did not increase further when longer constructs were used (Figure 4A). Hypoxia did not increase the activity of the shorter constructs pGL3*Vldlr*55 (–55 bp to ATG) or pGL3*Vldlr*123 (–123 bp to ATG) (Figure 4A). These results indicate the presence of a hypoxia-responsive element (HRE) between –180 and –123 bp. In silico analyses indicated the presence of a potential HIF-1α site between –162 and –158 bp. Mutation of this site within the pGL3*Vldlr*180 construct completely abolished the hypoxia-induced luciferase activity but did not change the basal activity seen in normoxia (Figure 4A). Thus we determined that the potential HIF-1α site constitutes the HRE in the *Vldlr* promoter.

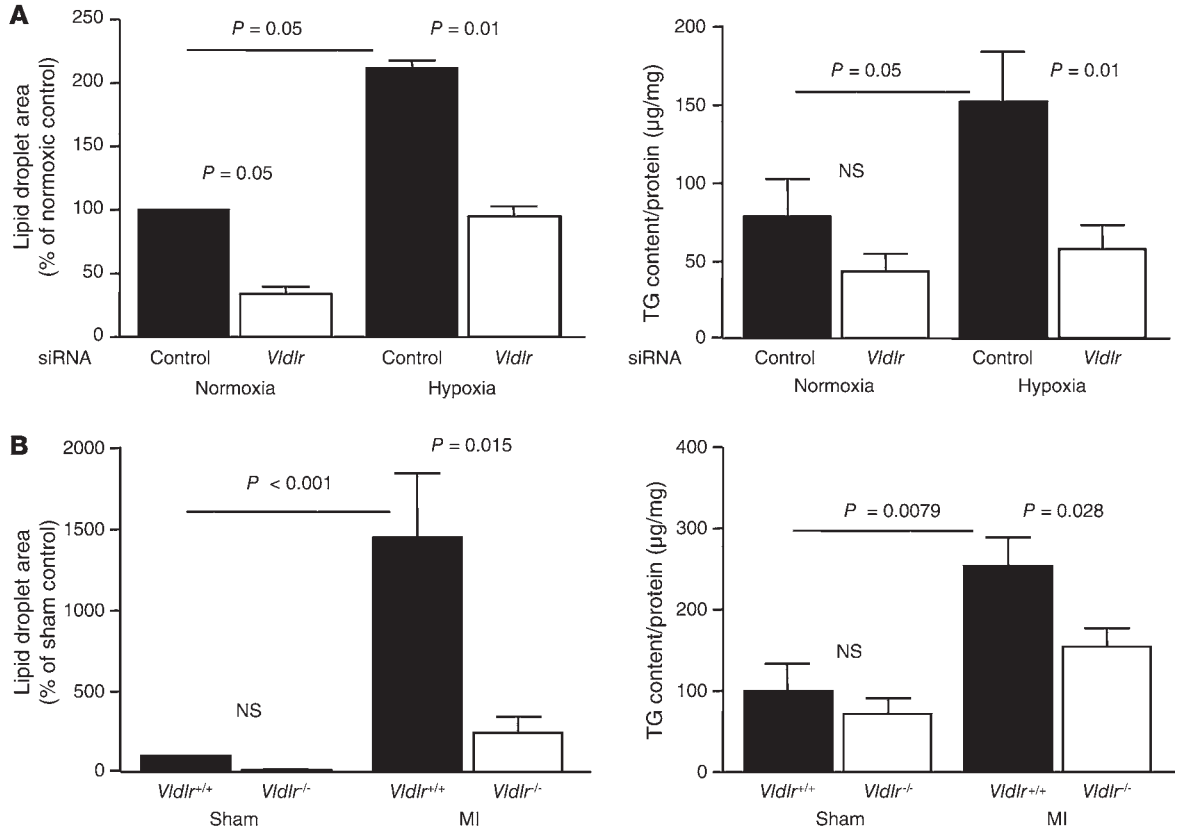

Figure 2

The VLDLR is required for triglyceride accumulation during hypoxia/ischemia in HL-1 cells and mouse hearts. (**A**) The total area of Oil Red O–stained lipid droplets (left) and triglyceride content (right) in HL-1 cells transfected with control siRNA or *Vldlr* #1 siRNA and incubated in normoxia or hypoxia for 8 hours ($n = 6$). Results using additional *Vldlr* siRNAs are presented in Supplemental Figure 4. (**B**) The total area of Oil Red O–stained lipid droplets (left) and triglyceride content (right) in heart tissue from $Vldlr^{+/+}$ mice or $Vldlr^{-/-}$ mice 6 hours after a sham operation or an experimentally induced myocardial infarction ($n = 7$–13). Results are shown as mean ± SEM.

These observations indicate that a potential HIF-1α site between –162 and –158 bp mediates the hypoxia-induced activation of the *Vldlr* promoter. To further address the importance of HIF-1α for the hypoxia-induced activity of the *Vldlr* promoter, we measured the relative luciferase activity of the constructs pGL3*Vldlr*55 and pGL3*Vldlr*180 in normoxia and hypoxia in cells transfected with control siRNA or siRNA to HIF-1α. The results demonstrated that knockdown of HIF-1α completely abolished the effect of hypoxia on the pGL3*Vldlr*180 construct but did not influence the pGL3*Vldlr*55 construct (Figure 4B). These data indicate that HIF-1α is essential for the activity of the HRE in the *Vldlr* promoter.

Hypoxia promotes VLDLR-mediated uptake of lipoproteins by endocytosis. It has been proposed that the VLDLR mediates uptake of triglyceride-rich lipoproteins by receptor-mediated internalization of lipoproteins (18, 19). In agreement, we observed clusters of VLDLR on the surface of hypoxic HL-1 cells, which internalized over time into a smooth membrane compartment (Supplemental Figure 6). We also showed that lipid accumulation in HL-1 cells induced by either hypoxia (Figure 5A) or *Vldlr* overexpression (Figure 5, B and C) was significantly reduced in lipoprotein-deficient medium, indicating a requirement for exogenous lipoproteins. Furthermore, hypoxia promoted the uptake of fluorescently labeled triglyceride-rich lipoproteins in HL-1 cells, and this response was abolished in HL-1 cells transfected with VLDLR siRNA (Figure 5, D and E). Thus, it is likely that VLDLR-mediated endocytosis of triglyceride-rich lipoproteins plays a role in hypoxia-induced lipid accumulation.

The VLDLR has also been reported to increase lipid accumulation by promoting the action of LPL (18, 20, 21), and we investigated whether hypoxia could promote lipid uptake by increasing the activity of LPL. We showed that the total LPL activity in HL-1 cells was not affected by hypoxia (Figure 5F). Furthermore, transfection of HL-1 cells with LPL siRNA resulted in a reduction in *Lpl* mRNA expression (Supplemental Figure 7) without an effect on the hypoxia-induced increase in lipid droplet area (Figure 5G and Supplemental Figure 7). Thus, LPL does not appear to be involved in hypoxia-induced lipid accumulation.

VLDLR expression correlates with lipid droplet accumulation in ischemic human hearts. To investigate the potential role of *VLDLR* expression in ischemia-induced lipid accumulation in the human heart, we compared ischemic left ventricle myocardial biopsies taken from patients scheduled for coronary bypass surgery with left ventricle myocardial biopsies from nonischemic hearts from patients undergoing aortic valve replacement. The results showed that *VLDLR* mRNA expression was significantly higher in the ischemic hearts (Figure 6A).

We also compared the ischemic heart biopsies with biopsies from nonischemic hearts from a larger cohort of patients who were recipients of heart transplants and similarly showed increased expression

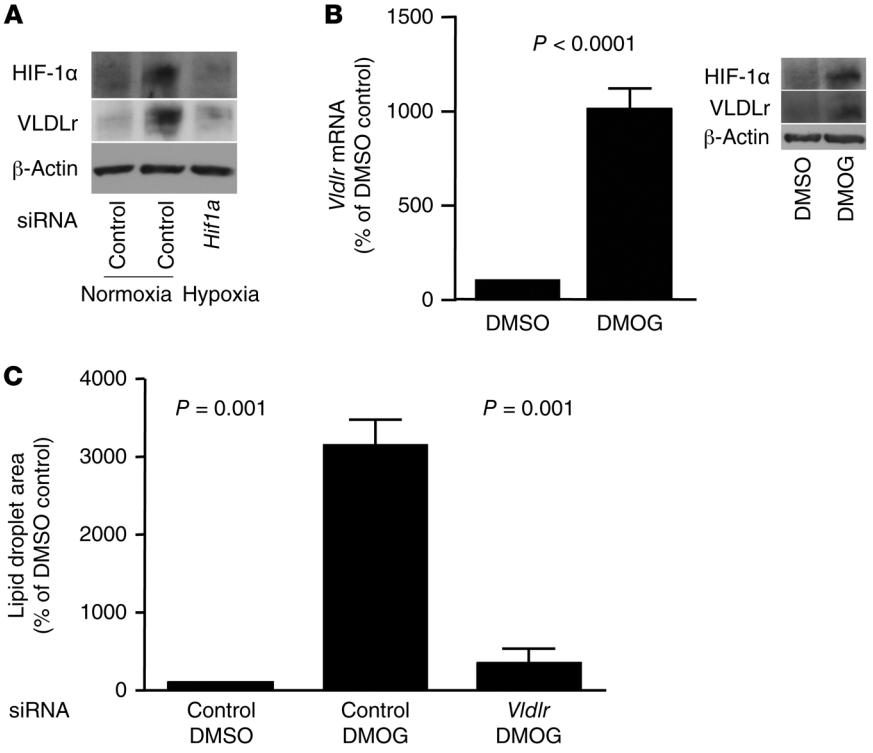

Figure 3
VLDLR expression is dependent on HIF-1α in HL-1 cells. (**A**) Representative immunoblots of HIF-1α, VLDLR, and β-actin in HL-1 cells transfected with control siRNA or *Hif1a* #1 siRNA and incubated in normoxia or hypoxia for 8 hours. (**B**) Real-time quantitative RT-PCR analysis of *Vldlr* mRNA expression ($n = 6$) (left) and representative immunoblots (right) of HIF-1α, VLDLR, and β-actin in normoxic HL-1 cells incubated with DMSO or the HIF-1α stabilizer DMOG (1 mmol/l) for 8 hours. (**C**) The total area of Oil Red O–stained lipid droplets in normoxic HL-1 cells transfected with control siRNA and incubated with DMSO (control), DMOG (1 mmol/l), or *Vldlr* #1 siRNA plus DMOG (1 mmol/l) for 8 hours ($n = 9$). Results are shown as mean ± SEM.

of the *VLDLR* in the group with the ischemic hearts (Figure 6A). A limitation with using the transplant biopsies is that the transplant recipients are treated with the immunosuppressant cyclosporine, which is a known inhibitor of protein synthesis. Indeed, we showed that levels of *VLDLR* mRNA and protein in HL-1 cells were reduced following incubation with cyclosporine for 1 week at a concentration that is observed in transplant recipients (1 μmol/l) (ref. 22 and Supplemental Figure 8), indicating that cyclosporine treatment may have suppressed the *VLDLR* expression in the transplanted hearts. However, *VLDLR* mRNA levels in the transplanted healthy hearts were similar to those measured in nonischemic left ventricle myocardial biopsies from patients undergoing aortic valve replacement (Figure 6A). Importantly, we also observed a strong positive correlation between expression of the *VLDLR* and the lipid droplet content in ischemic hearts (Figure 6B).

Improved survival after an acute myocardial infarction in Vldlr$^{-/-}$ mice. To elucidate the biological impact of the VLDLR-mediated lipid accumulation in response to ischemia, we investigated if knockout of the *Vldlr* could influence the survival after a myocardial infarction. We monitored *Vldlr$^{-/-}$* and *Vldlr$^{+/+}$* mice for up to 30 days after an experimentally induced acute myocardial infarction and, importantly, we observed increased survival in the *Vldlr$^{-/-}$* mice (Figure 7A). We also showed that although the total area at risk (a measure of the total ischemic region of the heart) was the same in ischemic hearts from *Vldlr$^{-/-}$* and *Vldlr$^{+/+}$* mice, the infarct area was reduced in *Vldlr$^{-/-}$* mice (Figure 7B).

The Vldlr promotes hypoxia/ischemia-induced ER stress. Hypoxia/ischemia is known to trigger ER stress, and recent evidence suggests that ER stress plays an important role in the progression of cardiovascular disease (15, 23). We therefore investigated whether the VLDLR is involved in promoting ER stress. Indeed, we showed that knockdown of the VLDLR in HL-1 cells decreased hypoxia-induced ER stress (Figure 8A). In addition, ER stress induced by thapsigargin resulted in increased expression of VLDLR (Figure 8, B and C). These results indicate that the VLDLR is important for hypoxia-induced ER stress, and they provide evidence for positive feedback between ER stress and the VLDLR.

We also investigated whether the ischemia-induced increase in VLDLR expression observed in vivo might be able to promote ER stress. Indeed, we showed that the expected increase in ER stress in heart tissue from mice after an experimentally induced myocardial infarction was abolished in *Vldlr$^{-/-}$* mice (Figure 9A). These data indicate the importance of the VLDLR in promoting ischemia-induced ER stress. Because ER stress promotes apoptosis (15), we therefore also investigated the effect of *Vldlr* knockout on apoptosis in the ischemic hearts. We first measured the expression of caspases (markers for the induction of apoptosis) and showed lower levels of caspase-3, -6, and -12 in ischemic hearts from *Vldlr$^{-/-}$* mice (Figure 9B). We also used the TUNEL assay to identify apoptotic cells and showed that the increase in TUNEL-positive cells in heart tissue from mice following an experimentally induced myocardial infarction was abolished in *Vldlr$^{-/-}$* mice (Figure 9C).

Reduced long-chain ceramides in the ischemic heart in Vldlr$^{-/-}$ mice. Accumulated triglycerides per se are unlikely to promote ER stress, and we therefore investigated whether altered levels of triglyceride degradation products in the ischemic *Vldlr$^{-/-}$* hearts might account for the reduced ER stress. However, we observed similar levels of total long-chain acyl-CoA, total diglycerides, and total ceramides in ischemic hearts from both groups of mice (Supplemental Figure 9), and thus we concluded that effects on total levels of lipid species could not explain the difference in ER stress between *Vldlr$^{+/+}$* and *Vldlr$^{-/-}$* mice.

A recent publication highlighting the importance of subspecies of ceramides for survival during lack of oxygen (24) prompted us to analyze ceramide subspecies in ischemic hearts from *Vldlr$^{+/+}$*

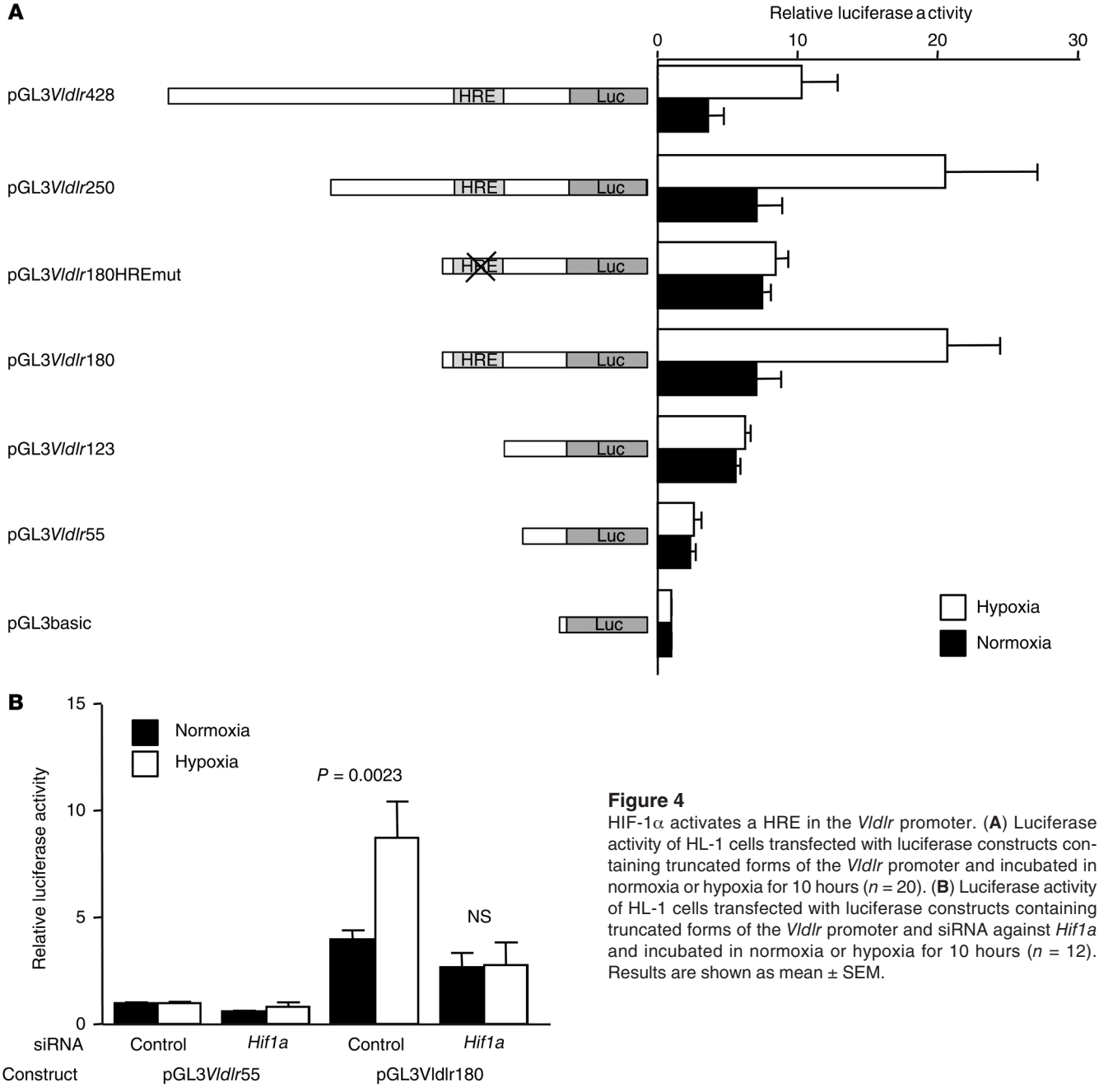

Figure 4
HIF-1α activates a HRE in the *Vldlr* promoter. (**A**) Luciferase activity of HL-1 cells transfected with luciferase constructs containing truncated forms of the *Vldlr* promoter and incubated in normoxia or hypoxia for 10 hours ($n = 20$). (**B**) Luciferase activity of HL-1 cells transfected with luciferase constructs containing truncated forms of the *Vldlr* promoter and siRNA against *Hif1a* and incubated in normoxia or hypoxia for 10 hours ($n = 12$). Results are shown as mean ± SEM.

and *Vldlr*$^{-/-}$ mice. We observed a decrease in ceramide species with longer acyl chains (ceramides C24–C26) in ischemic hearts from *Vldlr*$^{-/-}$ mice but found no change in the ceramide species with shorter chains (ceramides C20–C22) (Figure 10A and see Supplemental Table 3 for all ceramide subspecies). Furthermore, we showed that C24–C26 ceramides were the most abundant ceramide species in human ischemic left ventricle biopsies, with significantly higher levels compared with C20–C22 ceramides (Supplemental Figure 10A). Moreover, C24–C26 ceramides, but not C20–C22 ceramides, correlated positively with *Vldlr* mRNA expression (Supplemental Figure 10B). Finally, we incubated HL-1 cells with ceramides and showed that C24 but not C20–C22 ceramides induced ER stress (Figure 10B). These results indicate that the increase of ceramides C24–C26 seen in the ischemic hearts may participate in the induction of ER stress.

VLDLR antibodies inhibit ischemia-induced lipid accumulation and ER stress. Our results indicate that the VLDLR is a potential target for therapy against ER stress and apoptosis during ischemia, and we therefore investigated the therapeutic potential of blocking the VLDLR by injecting mice with antibodies against the VLDLR or saline during an experimentally induced myocardial infarction. We observed that antibody treatment significantly decreased both the lipid droplet area (Figure 11A) and ER stress (Figure 11B) and resulted in a strong tendency toward decreased apoptosis (Figure 11C) in ischemic hearts. These data provide further support for the role of the VLDLR in promoting both lipid accumulation and ER stress.

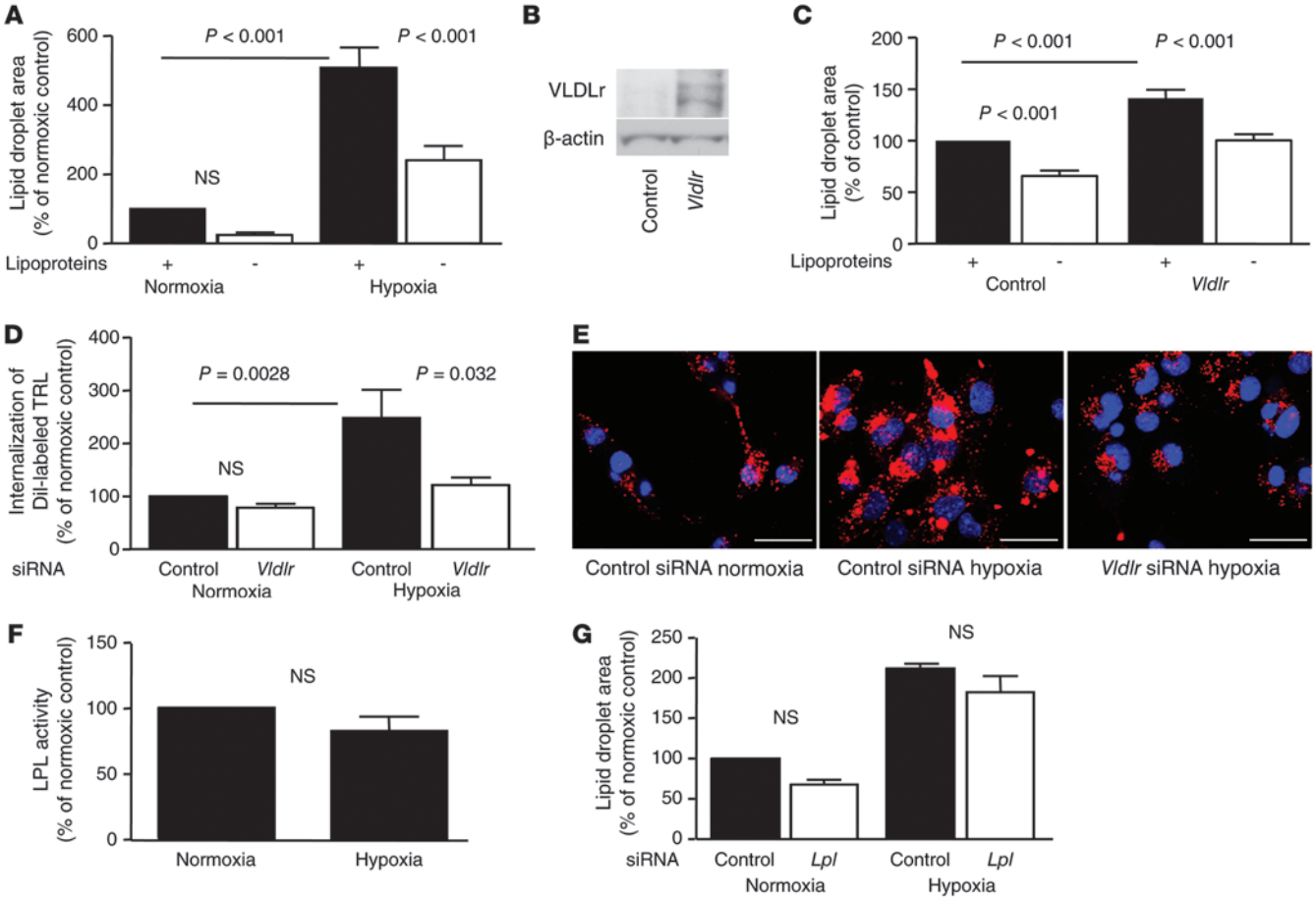

Figure 5

Hypoxia-mediated lipid accumulation in HL-1 cells requires exogenous lipoproteins and is mediated by endocytosis of triglyceride-rich lipoproteins (TRLs) through the VLDLR. (**A**) The total area of Oil Red O–stained lipid droplets in HL-1 cells incubated in normoxia or hypoxia for 8 hours in the presence or absence of exogenous lipoproteins (n = 20). (**B**) Representative immunoblot against antibodies to VLDLR or β-actin in HL-1 cells transfected with an empty vector (control) or a vector encoding *Vldlr*. (**C**) The total area of Oil Red O–stained lipid droplets in HL-1 cells transfected with an empty vector (control) or a vector encoding *Vldlr* and incubated in the presence or absence of exogenous lipoproteins (n = 10). (**D**) Internalization of TRLs labeled with a fluorescent probe (DiI) in HL-1 cells transfected with control siRNA or *Vldlr* #1 siRNA and incubated in normoxia or hypoxia for 8 hours (n = 24). (**E**) Representative micrographs of **D**. Scale bars: 50 μm. (**F**) The total LPL activity in HL-1 cells incubated in normoxia or hypoxia for 8 hours (n = 6). (**G**) The total area of Oil Red O–stained lipid droplets in HL-1 cells transfected with control siRNA or *Lpl* #1 siRNA and incubated in normoxia or hypoxia for 8 hours (n = 6). Results using additional *Lpl* siRNAs are presented in Supplemental Figure 7. Results are shown as mean ± SEM.

Discussion

In this article, we demonstrate the importance of the VLDLR in hypoxia/ischemia-induced lipid accumulation in HL-1 cardiomyocytes and mouse hearts, and we also provide evidence indicating a role for the VLDLR in human ischemic heart tissue. Importantly, we show that survival after an experimentally induced myocardial infarction is improved in *Vldlr*$^{-/-}$ mice, which may be explained by the observed reduction in ischemia-induced ER stress and apoptosis in *Vldlr*$^{-/-}$ mouse hearts. Finally, treatment with antibodies to the VLDLR indicates that this receptor is a potential target for the treatment of ER stress during myocardial ischemia.

The hypoxia-induced accumulation of triglycerides in HL-1 cells might potentially be explained by increased uptake of fatty acids due to increased transport into the cell. This was supported by our observation of an increased uptake of fatty acids in hypoxic HL-1 cells. However, we show that hypoxia did not increase the expression of FATP, CD36, or FABP, which are well known to participate in fatty acid uptake. Hypoxia has been shown to promote the relocalization of CD36 from a storage form in the interior of the cell to the plasma membrane, where it is involved in the uptake of fatty acids (16), and we therefore used FACS analyses to investigate whether this also occurs in HL-1 cells. We did not detect a hypoxia-induced increase of CD36 in the plasma membrane, but it is possible that different times of exposure to hypoxia might explain the discrepancy. We incubated cells in hypoxia for 8 hours, whereas CD36 relocalization was observed after 15 minutes hypoxia in the previous study (16).

Although relocalization of CD36 cannot explain the increased accumulation of triglycerides seen in our study, our data should not be used to rule out the basic principle of relocalization of CD36 and the significance of this transporter for the accumulation of lipids in the myocardium. Indeed, it has been demonstrated that CD36 deficiency might rescue the lipotoxic cardiomyopathy induced by

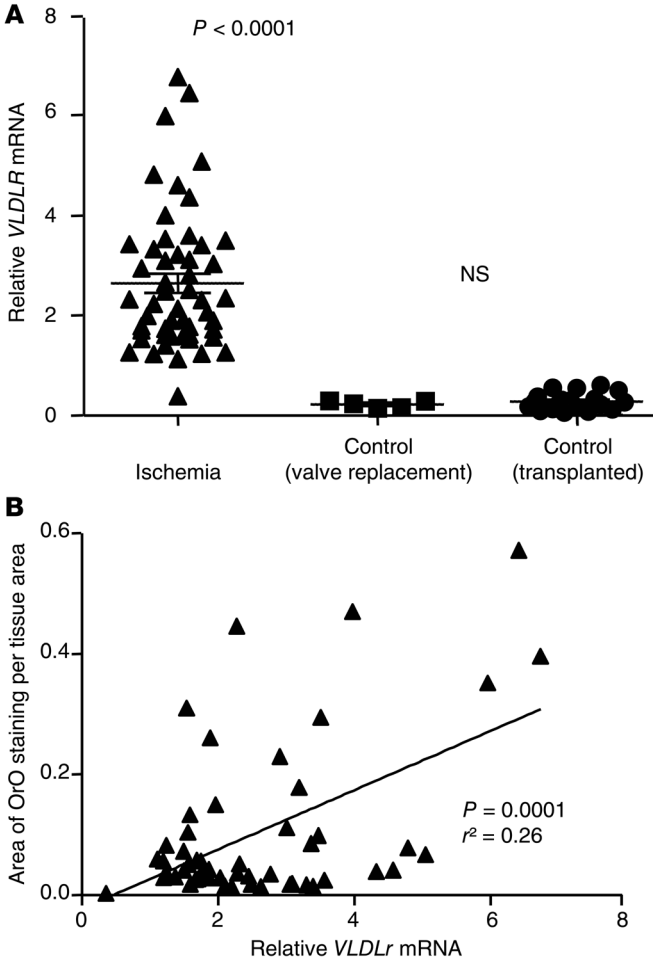

Figure 6
VLDLR expression is higher in ischemic compared with nonischemic human hearts and correlates with accumulation of lipid droplets. (**A**) Real-time quantitative RT-PCR analysis of *VLDLR* mRNA expression in human biopsies from ischemic left ventricles (left; $n = 52$), control biopsies from nonischemic left ventricles taken from patients undergoing aortic valve replacement (middle; $n = 5$), and control biopsies from transplanted nonischemic left ventricles (right; $n = 19$). (**B**) The relation between *VLDLR* mRNA expression and the total area of Oil Red O–stained (OrO-stained) lipid droplets in biopsies from ischemic human hearts.

overexpression of PPARα in the myocardium (25). Such overexpression of PPARα has been shown to induce a cardiac phenotype that mimics that induced by diabetes mellitus, in which the heart relies almost exclusively on fatty acid oxidation for energy production and has a severely decreased uptake and oxidation of glucose (26). In our study, hypoxia promoted a shift away from oxidation of fatty acids toward glycolysis, in agreement with earlier studies (3, 4). Fatty acids that enter the cells are not used for energy production but are instead converted to lipids. In addition, glucose uptake and glycolysis are promoted. The phenotype induced by hypoxia/ischemia thus differs from the situation in mice with overexpressed PPARα (26).

Neither the increased uptake of fatty acids nor the metabolic changes induced by hypoxia in our study were sufficient to induce lipid accumulation when the VLDLR was knocked down in HL-1 cells or knocked out or blocked by antibodies in heart tissue, highlighting the importance of the VLDLR in lipid accumulation. Our results thus indicate that increased expression of the VLDLR is essential for the accumulation of triglycerides in hypoxic HL-1 cells and ischemic myocardium in mice.

The hypoxia-induced increase in VLDLR expression is likely a general phenomenon, as hypoxia has previously been shown to increase *Vldlr* mRNA expression in Müller cells (27) and human monocytes (28). In agreement with those findings, we demonstrate that hypoxia induced an increase in the VLDLR expression in a number of cell lines. We also show that HIF-1α was important for the hypoxia-induced expression of the VLDLR in HL-1 cells. Analysis of the VLDLR promoter showed a HRE between –162 and –158 bp, and knockdown experiments showed that HIF-1α was essential for the activity of this HRE. Thus we conclude that HIF-1α mediates the hypoxia-induced expression of the VLDLR through a HRE in the promoter region of the gene.

Our investigations into how hypoxia promotes lipid accumulation indicate that the VLDLR likely mediates uptake of triglyceride-rich lipoproteins by endocytosis, in agreement with previous studies (18, 19). The VLDLR has also been reported to promote lipid accumulation by co-operating with LPL (18, 20, 21). However, we show that hypoxia did not affect LPL activity and that *Lpl* knockdown did not influence the hypoxia-induced lipid accumulation in HL-1 cells, in agreement with a previous study showing that *Lpl* knockout does not influence cardiac lipid accumulation (29). We therefore conclude that LPL is not essential for the VLDLR-dependent accumulation of triglycerides during hypoxia/ischemia.

We also showed that *VLDLR* expression was higher in biopsies from the left ventricle of ischemic human hearts compared with biopsies from nonischemic left ventricles. Furthermore, we observed a significant relationship between the *VLDLR* expression and the pool of lipid droplets in ischemic hearts. These observations indicate that ischemia is also associated with increased expression of the *VLDLR* in the human heart. Moreover, although these types of analyses cannot provide information about mechanisms, these associations are consistent with a link between *VLDLR* expression and accumulation of neutral lipids in the ischemic human heart.

One of our major aims was to determine whether lipid accumulation is detrimental to the ischemic heart. We therefore tested the hypothesis that increased VLDLR expression in the heart is coupled to increased risk of death shortly after a myocardial infarction in mice. Our results showed improved survival in $Vldlr^{-/-}$ mice compared with $Vldlr^{+/+}$ mice in the early phase of an experimentally induced acute myocardial infarction. Echocardiographic analysis of $Vldlr^{-/-}$ and $Vldlr^{+/+}$ mice at rest and during dobutamine stress showed some differences between the groups, but the changes were generally small and there was no difference in fractional shortening (Supplemental Table 4). However, the $Vldlr^{-/-}$ mice failed to increase their cardiac index during stress and had a significantly lower cardiac index compared with $Vldlr^{+/+}$ mice during this stress. These observations may, if anything, indicate that the myocardial function of $Vldlr^{+/+}$ mice is better than that of $Vldlr^{-/-}$ mice at baseline. Therefore, it is unlikely that these observations can explain the improved survival of the $Vldlr^{-/-}$ mice. We further examined whether $Vldlr^{-/-}$ mice are resistant to pathological remodeling after myocardial infarction by analyzing the left ventricular mass at baseline and 1 and 6 weeks after an induced myocardial infarction using echocardiography.

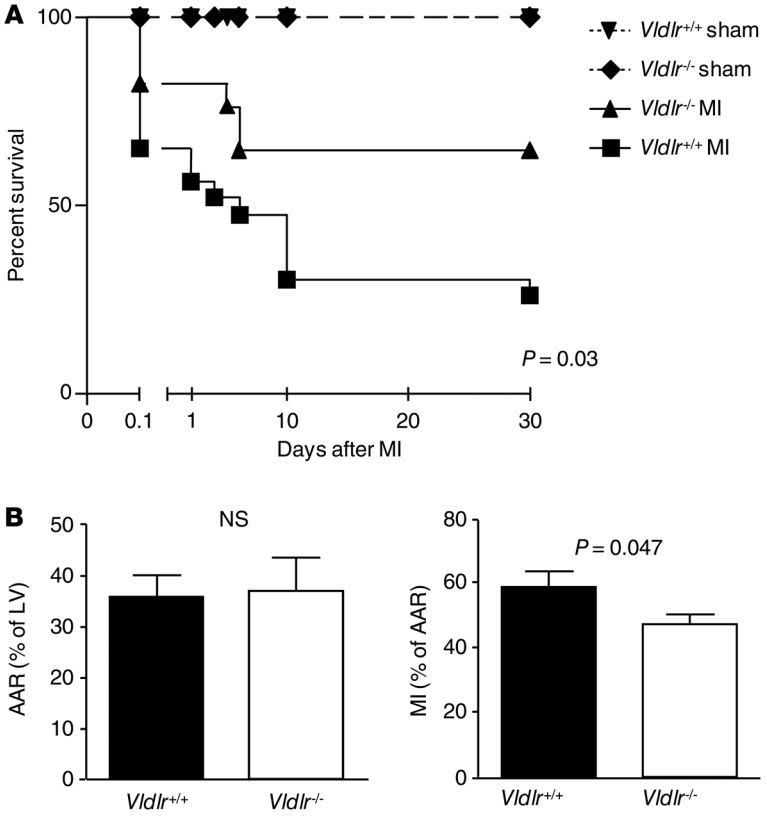

Figure 7
Vldlr knockout improves survival and reduces infarct area and apoptosis in the heart after an experimentally induced acute myocardial infarction in mice. (**A**) The survival of $Vldlr^{+/+}$ and $Vldlr^{-/-}$ mice after a sham operation or an experimentally induced myocardial infarction (n = 20). (**B**) The area at risk (AAR) in the left ventricle (left) and infarct area (right) in $Vldlr^{+/+}$ and $Vldlr^{-/-}$ mouse hearts 6 hours after an experimentally induced myocardial infarction (n = 10). Results are shown as mean ± SEM.

The results did not show any significant difference in left ventricular mass between $Vldlr^{-/-}$ and $Vldlr^{+/+}$ mice (data not shown). We also weighed the left ventricles of hearts from $Vldlr^{-/-}$ and $Vldlr^{+/+}$ mice 6 weeks after an induced myocardial infarction and did not observe any significant difference (data not shown). Thus, the results do not support that $Vldlr^{-/-}$ mice are resistant to ischemia-induced pathological remodeling after a myocardial infarction.

The majority of the deaths occurred within the first 1–3 days. Lipid droplet area was significantly increased in heart tissue from $Vldlr^{+/+}$ mice 6 hours after the induction of a myocardial infarction (Figure 2B), and thus the difference in lipid droplet accumulation was established when most of the deaths occurred. The ischemia-induced accumulation of lipid droplets decreased with time, but a difference between the lipid droplet area in $Vldlr^{+/+}$ and $Vldlr^{-/-}$ mice remained 1 week after the myocardial infarction (Supplemental Figure 11).

It is known that the size of the infarct area is a key determinant of the outcome of an acute myocardial infarction (30, 31), and here we showed that *Vldlr* knockout also reduced infarct area in mouse hearts after an experimentally induced myocardial infarction. There were no differences in the total area at risk of infarct between $Vldlr^{+/+}$ and $Vldlr^{-/-}$ mice, excluding variations in the experimental system as an explanation for this result. We thus propose that this reduced infarct size may be a major contributor to the improved survival in $Vldlr^{-/-}$ mice.

Although the correlation between *VLDLR* expression and the pool of lipid droplets in ischemic human hearts remained when patients with diabetes were excluded, it is possible that VLDLR-mediated lipid accumulation is of particular importance in patients with diabetes and/or obesity. These patients have increased myocardial levels of triglycerides even under normoxic conditions (7, 32–35), and their high myocardial triglyceride content has been associated with impaired left and right ventricle function (34, 35). In these cases, uptake of fatty acids via CD36 seems to be important (25). These patients may also have an increased storage of triglycerides during acute ischemia because they overproduce triglyceride-rich lipoproteins (36), which are ligands of the VLDLR. The increased VLDLR-mediated lipid accumulation may partly explain why patients with type 2 diabetes have an increased risk of sudden cardiac death after myocardial infarction (37).

Accumulation of lipids in the cell and exposure to fatty acids have been linked to the development of ER stress (15, 38–40). Moreover, hypoxia/ischemia has been shown to promote ER stress (15, 23), which has been proposed to play an important role in the progression of ischemic heart disease (15). We therefore investigated whether the detrimental effect of the VLDLR in the ischemic heart might be explained by a link between the VLDLR and ER stress. In agreement with our hypothesis, we showed that the VLDLR promoted hypoxia-induced ER stress in HL-1 cells and mouse heart tissue. Interestingly, we observed that ER stress also induced expression of the VLDLR in HL-1 cells. This indicates that there is a feedback loop in which the hypoxia-induced increase in VLDLR results in ER stress, which in turn promotes the expression of the VLDLR. In this way, the effect of hypoxia on ER stress can be amplified.

Although our data clearly show that the VLDLR promotes increased accumulation of triglycerides in ischemic heart tissue, accumulated triglycerides per se are likely to be inert and thus not directly lipotoxic. Indeed, promotion of lipid droplets in macrophages has been shown to prevent lipotoxicity (12). However, increased triglyceride accumulation is likely to be associated with increased accumulation of degradation products, including diglycerides, fatty acids, and products of fatty acids such as ceramides, which have been linked to the induction of apoptosis (reviewed in ref. 41). We thus hypothesized that increased accumulation of triglycerides would promote ER stress by increasing the availability of degradation products in ischemic hearts from $Vldlr^{+/+}$ compared with $Vldlr^{-/-}$ mice.

To address our hypothesis, we first investigated the effect of *Vldlr* knockout on total levels of lipid species in the ischemic heart, but we did not observe any differences that could explain reduced ER stress. However, we demonstrated lower levels of C24–C26 ceramides (and similar levels of C20–C22 ceramides) in ischemic heart tissue from $Vldlr^{-/-}$ compared with $Vldlr^{+/+}$ mice. Long-chain ceramides have been shown to accumulate in hearts of mice exposed to hypoxia from birth (42), but the importance of individual ceramide subspecies on ER stress has not been previously investigated. However, recent results indicate that the fatty acid chain length of ceramides is an important

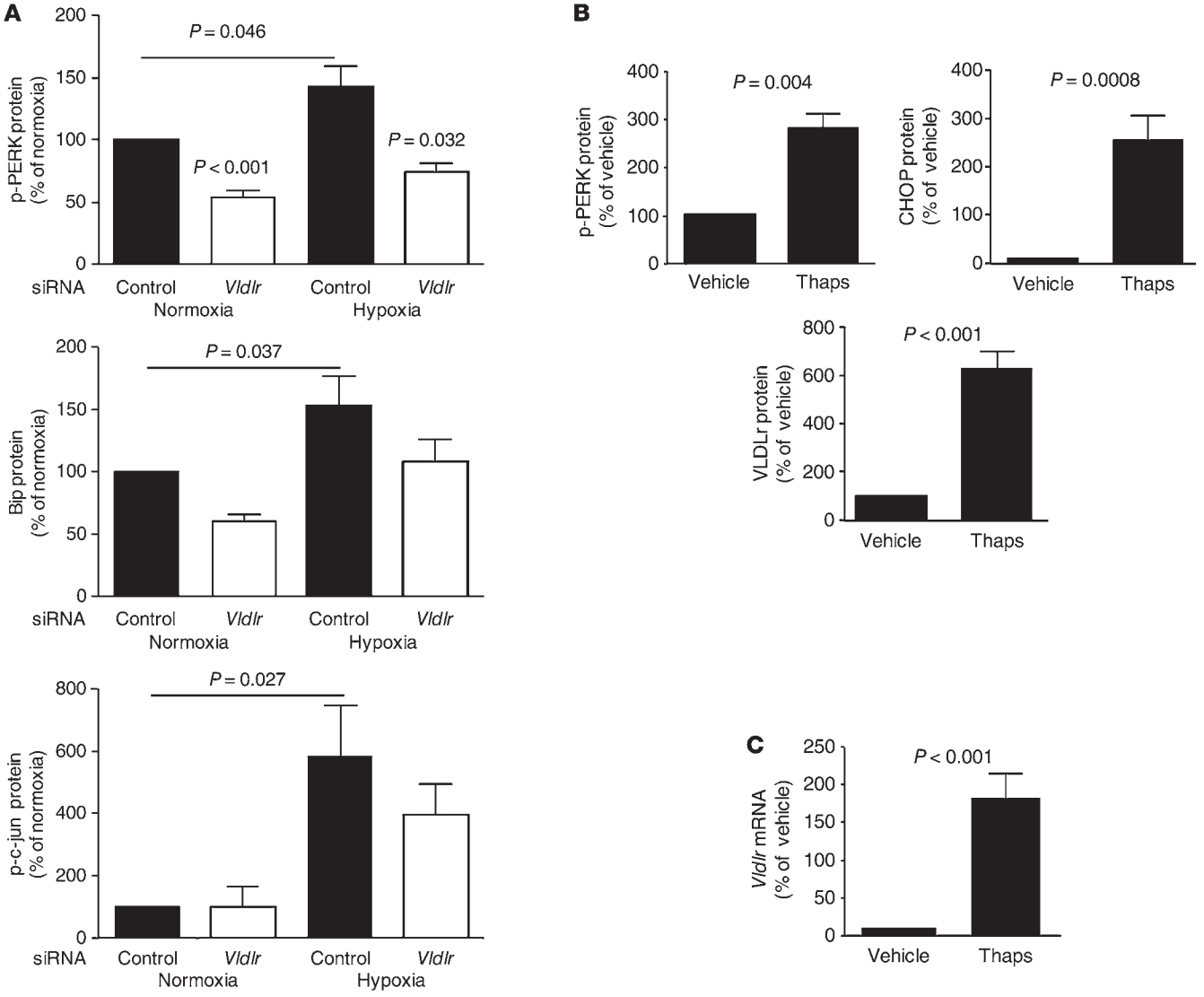

Figure 8

Hypoxia-induced ER stress in HL-1 cells is decreased by *Vldlr* knockdown. ER stress also induces *Vldlr* expression in HL-1 cells. (**A**) Quantification of immunoblots against markers for ER stress in HL-1 cells transfected with control siRNA or *Vldlr* siRNA and incubated in normoxia or hypoxia for 8 hours ($n = 6$). (**B** and **C**) Quantification of immunoblots against markers for ER stress or the VLDLR (**B**) and real-time quantitative RT-PCR of *Vldlr* mRNA (**C**) in HL-1 cells incubated with vehicle or thapsigargin (Thaps, 1 μmol/l) for 12 hours ($n = 6$). Results are shown as mean ± SEM.

determinant of the biological effect mediated by the bioactive lipid. Thus, C24–C26 ceramides have been shown to mediate the death of a *Caenorhabditis elegans* mutant that fails to withstand asphyxia, whereas ceramides with shorter chains have the opposite effect (ref. 24 and comments in ref. 43). This study prompted us to investigate the relative effect of longer- versus shorter-chain ceramides in HL-1 cells, and we showed that the C24 ceramide induced ER stress, whereas the shorter chain (C20–C22 and C16) ceramides had no effect. This indicates that the hypoxia/ischemia-induced ER stress might at least in part be explained by the increased level of C24–C26 ceramides.

The involvement of ER stress in diseases such as neurodegenerative diseases, type 1 and 2 diabetes, and cardiovascular disease (15, 23, 44) indicate that it is important to consider therapeutic strategies to limit the damage caused by ER stress. Our data showing that the VLDLR has a central role in the development of ER stress and apoptosis in the ischemic heart suggested the therapeutic potential of targeting the VLDLR to reduce the effects of these potentially damaging processes during ischemia. We therefore injected mice with antibodies against the VLDLR during the induction of an experimental myocardial infarction and showed that blockade of the VLDLR decreased both the accumulation of lipids and the ER stress and showed a strong trend toward a reduction in apoptosis in ischemic hearts. These results complement the genetic deletion experiments and overcome concerns about potential developmental issues with genetic deletion of the *Vldlr*. They also provide a context for a therapeutic approach to acute ischemia of the heart by blocking the VLDLR.

In summary, this is to our knowledge the first study to show increased expression of VLDLR protein in response to hypoxia/ischemia of cardiomyocytes and mouse hearts. More importantly, we also demonstrate that this receptor mediates the accumulation

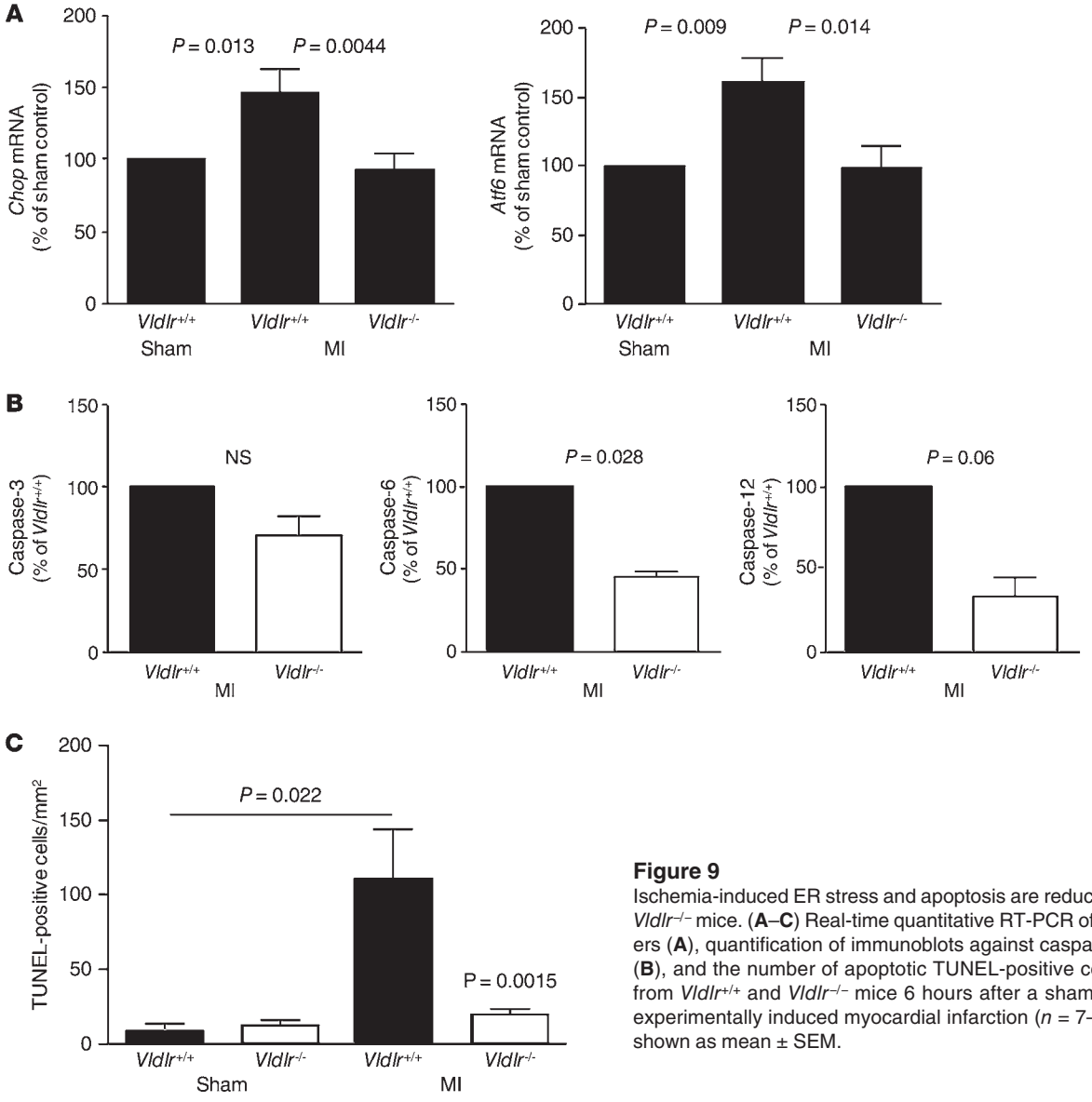

Figure 9
Ischemia-induced ER stress and apoptosis are reduced in hearts from *Vldlr*$^{-/-}$ mice. (**A**–**C**) Real-time quantitative RT-PCR of ER stress markers (**A**), quantification of immunoblots against caspase-3, -6, and -12 (**B**), and the number of apoptotic TUNEL-positive cells (**C**) in hearts from *Vldlr*$^{+/+}$ and *Vldlr*$^{-/-}$ mice 6 hours after a sham operation or an experimentally induced myocardial infarction (n = 7–13). Results are shown as mean ± SEM.

of lipids in the myocardium during ischemia, resulting in reduced survival following an acute myocardial infarction. We propose that survival during acute ischemia is increased in *Vldlr*$^{-/-}$ mice because of reduced ER stress, which leads to decreased apoptosis and a decreased infarct area. Our results also indicate that the VLDLR is a potential target for therapy to reduce mortality in the early phase of a myocardial infarction.

Methods

Induction of myocardial infarction and preparation of tissue sections. Myocardial infarction in C57BL/6 *Vldlr*$^{+/+}$ and *Vldlr*$^{-/-}$ mice (The Jackson Laboratory) was induced by permanent ligation of the left coronary artery as described previously (45). For the VLDLR antibody experiments, C57BL/6 *Vldlr*$^{+/+}$ mice were injected intraperitoneally during surgery (46) with 100 μl antibodies (2.3 μg/μl) or saline solution. The antibodies have been described previously (47, 48). Mice were fed ad libitum but fasted 4 hours before the operation, and water was available ab libitum during the whole procedure. With the exception of the *Vldlr*$^{+/+}$ and *Vldlr*$^{-/-}$ mice in the survival study, mice were killed with an overdose of isoflurane 6 hours after occlusion (i.e., in the middle to late afternoon). The hearts were removed, briefly rinsed in PBS, embedded in OCT compound, frozen in liquid nitrogen, and stored at –80°C until analysis. Areas at risk of infarction and infarct size were measured using the ImageJ software after staining with Evan's Blue and triphenyltetrazolium chloride. The experiments were approved by the Gothenburg Ethical Committee on Animal Experiments.

Human heart biopsies. Ischemic heart biopsies were obtained from 79 patients scheduled for coronary artery bypass grafting surgery. Angiograms of these patients revealed significant coronary atherosclerosis within the left anterior descending artery and/or the left coronary artery and/or branches from these vessels, and needle biopsies were taken from the left ventricle region affected by ischemia. Of 79 biopsies, 27 were excluded because the biopsy was too small, there was too little RNA, or the RNA was of unacceptable quality. Therefore, 52 biopsies were analyzed for *Vldlr* expression and lipid content. The subjects had a mean ± SEM BMI of 27.6 ± 3.8 (median 26.4), and ten subjects had type 2 diabetes (further characteristics of these subjects are presented in Supplemental Table 5). Exclusion of diabetic subjects did not affect the statistical outcome.

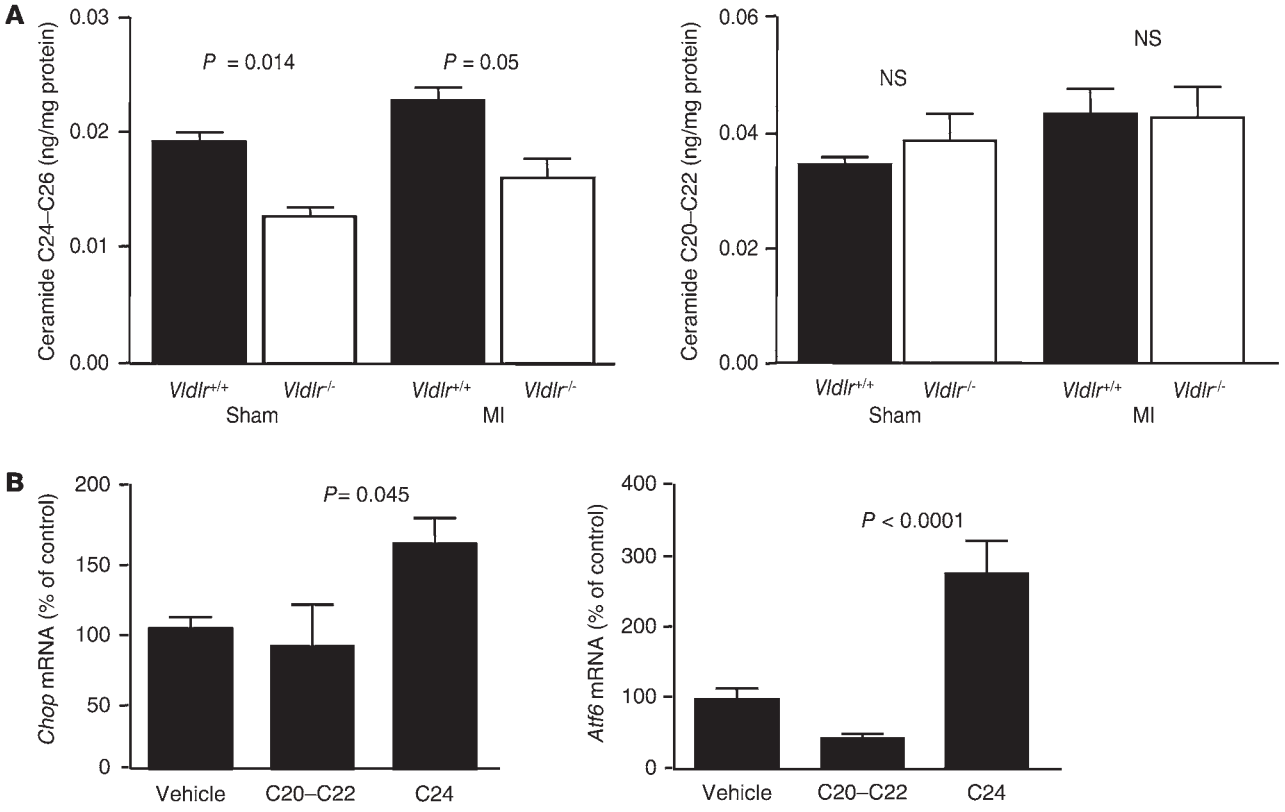

Figure 10
Long-chain ceramides (C24–C26) are reduced in *Vldlr*$^{-/-}$ mice and induce ER stress when added to HL-1 cells. (**A**) Quantification of the total amount of ceramides C24–C26 and C20–C22 in heart tissue from *Vldlr*$^{+/+}$ and *Vldlr*$^{-/-}$ mice 6 hours after a sham operation or an experimentally induced myocardial infarction (n = 7–13) (**B**) Real-time quantitative RT-PCR analysis of ER stress markers in HL-1 cells incubated with vehicle, ceramides C20–C22, or ceramide C24 (3 μmol/l) for 8 hours (n = 6). Results are shown as mean ± SEM.

Nonischemic heart biopsies from the left ventricle were also obtained from 3 women and 2 men undergoing aortic valve replacement. These subjects all had angiography-verified absence of coronary artery disease in any major myocardial coronary artery branch. Nonischemic left ventricle myocardial biopsies were obtained from 19 subjects 4 months after orthotopic heart transplantation as a routine check for graft rejection (49). Only biopsies without signs of rejection were used. The experimental protocol was approved by the Gothenburg Regional Ethics Committee and performed according to the Declaration of Helsinki. All patients gave written informed consent.

HL-1 cells and incubation in hypoxia. The HL-1 cardiomyocyte cell line was a gift from W. Claycomb (Louisiana State University Medical Center, New Orleans, Louisiana, USA). The cells were cultured as described previously (50) and incubated in supplemented Claycomb media (50) at 21% oxygen (normoxia) or 1% oxygen (hypoxia) for 8 hours. We demonstrated that the expression of the VLDLR or the accumulation of lipid droplets in the HL-1 cells was not influenced by norepinephrine or retinoic acid (Supplemental Figure 12). Potentially cytotoxic effects of the cell culture conditions were measured using the trypan blue exclusion test (51). Incubation in hypoxia for 8 hours did not alter the viability of HL-1 cells (Supplemental Figure 13).

Measurement of lipid droplet area and triglyceride content. To determine the lipid droplet area in heart tissue, frozen mouse hearts and human heart biopsies were cryosectioned in 8-μm slices, transferred to polysine glass slides, and stained with Oil Red O as previously described (52). The slides were mounted with gelatin-glycine solution, photographed with a Zeiss Axioplan microscope, and the area of Oil Red O staining per tissue area was determined as previously described (53). The lipid droplet area in HL-1 cells was also determined by staining with Oil Red O, as described in ref. 54. The intracellular triglyceride content in heart tissue and HL-1 cell lysates was measured as previously described (55).

Measurement of lipid classes in HL-1 cells. For analysis of lipid classes in HL-1 cells (Supplemental Table 1), lipid classes were extracted from HL-1 cells as described previously (56) and quantified using straight-phase HPLC with evaporative light scattering detection (57).

FACS. HL-1 cells in suspension were incubated with Fc block (2.4G2; BD Biosciences) for 20 minutes at room temperature to avoid nonspecific binding via Fc receptor interactions. Staining was performed by incubating the selected antibodies for 45 minutes at 4°C diluted in FACS buffer (1% FCS, 0.1% NaAz, 0.5% EDTA), followed by washing and secondary detection antibody incubation. The following antibodies were used for VLDLR analysis: monoclonal goat anti-mouse VLDLR antibody (R&R Systems) at 200 μl/ml with secondary antibody APC-conjugated donkey anti-goat F(ab′)$_2$ antibody (Santa Cruz Biotechnology) at 40 μg/ml. For CD36 analysis, APC-conjugated monoclonal rat anti-mouse CD36 antibody (AbCam) at 40 μg/ml was used. After the staining procedure, the cells were resuspended in 200 μl of FACS buffer and kept on ice. From each sample, 1–5 × 10^5 cells were collected in a FACS Canto II equipped with FACS Diva software (BD Biosciences). The cells were gated based on the "fluorochrome minus one" setting when needed (58). All analyses were performed using the FlowJo software (Three Star Inc.).

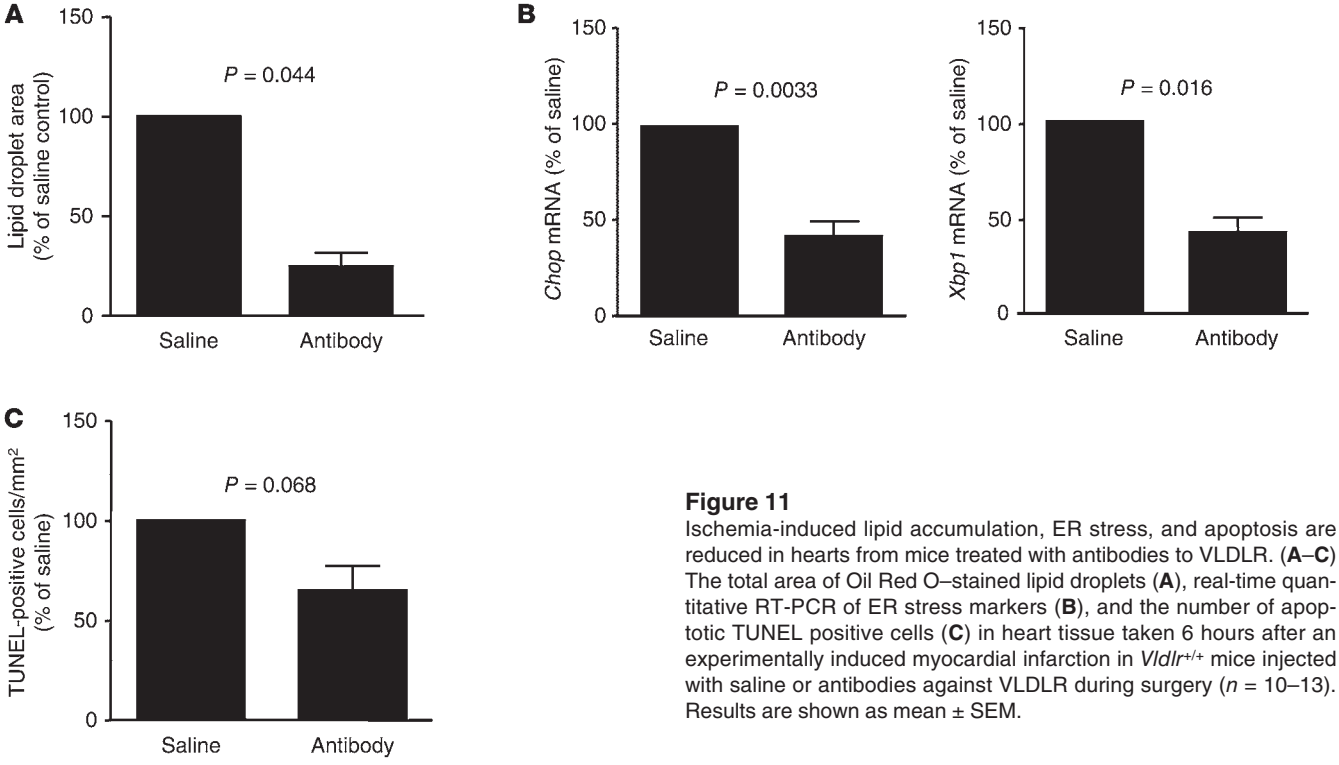

Figure 11
Ischemia-induced lipid accumulation, ER stress, and apoptosis are reduced in hearts from mice treated with antibodies to VLDLR. (**A**–**C**) The total area of Oil Red O–stained lipid droplets (**A**), real-time quantitative RT-PCR of ER stress markers (**B**), and the number of apoptotic TUNEL positive cells (**C**) in heart tissue taken 6 hours after an experimentally induced myocardial infarction in *Vldlr*$^{+/+}$ mice injected with saline or antibodies against VLDLR during surgery (n = 10–13). Results are shown as mean ± SEM.

Metabolic studies. To measure uptake of free fatty acids, HL-1 cells were incubated in hypoxia or normoxia for times indicated in the figures with medium containing 0.5 μCi/ml of ^{3}H-oleic acid (PerkinElmer) crosslinked to albumin. The recovery of radioactivity in the HL-1 cells was measured by scintillation counting. β-Oxidation in HL-1 cells was determined as previously described (59). Briefly, cells were incubated in hypoxia or normoxia for 8 hours with medium containing 0.5 μCi/ml ^{3}H-palmitate with 1% fatty acid–free BSA and 110 μmol/l palmitic acid for the final 105 minutes. The medium was then collected and fatty acids were precipitated 3 times with perchloric acid and a high concentration of BSA. The unprecipitated medium (containing metabolites of β-oxidation) was then analyzed for radioactivity. MitoTracker staining for mitochondria (MitoTracker Green) and metabolically active mitochondria (MitoTracker Red; Invitrogen) was performed according to the manufacturer's protocol. Briefly, cells were cultured on coverslips for 8 hours in normoxia or hypoxia before addition of MitoTracker (50 nmol/l) diluted in prewarmed culture medium. After a further 30 minutes, the cells were washed, fixed in 4% paraformaldehyde, and mounted on glass slides. Slides were photographed with a Zeiss Axioplan microscope under fluorescent light. The number of active and total mitochondria was quantified using the BioPix software. To investigate the uptake of glucose, HL-1 cells were incubated in hypoxia or normoxia for 8 hours with the addition of 25 μCi/ml 2-deoxy-D-[^{14}C] glucose (Amersham Biosciences) 15 minutes before the end of the incubation. This method was performed as previously described (60), with the adjustments described in ref. 54.

Analysis of gene and protein expression. Total RNA was isolated from cells and homogenized mouse and human heart tissue using the RNeasy Mini Kit (Qiagen). cRNA synthesized from HL-1 cell mRNA was hybridized to microarrays according to the manufacturer's instructions and analyzed using an Affymetrix gene array (Moe 430 2.0) (54). For real-time quantitative RT-PCR analysis, we analyzed cRNA synthesized from total RNA from HL-1 cells, mouse heart tissue, or human biopsies using cDNA archive kit (Applied Biosciences), and results were normalized against *18S*. Immunoblots were performed as described previously (61), and protein levels were normalized against β-actin.

Immunohistochemistry. VLDLR expression in HL-1 cells was assessed by immunohistochemistry as previously described (61).

Transfection of HL-1 cells. The siRNAs used are shown in Supplemental Table 6 and were purchased from Applied Biosciences. They were transfected into HL-1 cells using Lipofectamine 2000 (Invitrogen) (62) 48 hours before analyses. For hypoxia experiments, HL-1 cells were incubated in hypoxia for the final 8 hours of the 48-hour siRNA incubation. A vector expressing human *Vldlr* was a gift from G.W. Rebeck (Georgetown University, Washington, DC, USA) (63) and was transfected into HL-1 cells using Lipofectamine 2000 twenty-four hours before analysis.

Vldlr expression in different cell types. Human aortic endothelial cells (cc2535) and human aortic smooth muscle cells (cc2571) were from In Vitro and were grown according to the manufacturer's protocol. Human satellite cells (a gift from A. Rustan, University of Oslo, Oslo, Norway) were differentiated into myotubes as previously described (64). NIH-3T3 cells were cultured as recommended by the American Type Culture Collection, and L6 cells were a gift from A. Klip (The Hospital for Sick Children, Toronto, Ontario, Canada) and grown as previously described (65). The cells were incubated at 21% oxygen (normoxia) or 1% oxygen (hypoxia) for 24 hours as previously described (66), prior to real-time quantitative RT-PCR analysis of *Vldlr* expression.

Promoter constructs. The pGL3 *Vldlr* luciferase plasmid (67), containing the proximal 2,590 bp of the mouse *Vldlr* promoter, was used to make a series of successive 5′ deletion constructs using standard cloning techniques. The mutant promoter pGL3 *Vldlr* 180HREmut was made by exchanging the putative HRE sequence GCGTG at –162 to –158 to G**GAT**C (in which bold text indicates alterations).

Transient transfection and reporter gene assay. HL-1 cells were transiently transfected with promoter constructs using Lipofectamine LTX and PLUS reagent (Invitrogen) according to the manufacturer's instructions. Briefly, cells were seeded in 12-well plates, transfected with 2.4 μg promoter construct and 0.1 μg pCMV-RL (Promega). The cells were harvested 48 hours after transfection (and incubated in hypoxia where indicated in the figure

legends for the final 10 hours). The cells were then washed once with ice-cold PBS, harvested in 100 μl lysis buffer, freeze-thawed 3 times, and then analyzed using Dual-Luciferase Reporter Assay System (Promega) according to the manufacturer's instructions.

Immunoelectron microscopy. HL-1 cells cultured on Thermanox coverslips (Nunc) were washed 3 times with PBS at 4°C and incubated on ice for 2 hours with 1:200 goat anti-VLDLR primary antibody (R&D Systems). The cells were then washed 3 times with PBS at 4°C, incubated on ice for 1 hour with the secondary antibody (donkey anti-goat IgG conjugated with 25-nm colloidal gold antibody; British Biocell International), and again washed 3 times with PBS at 4°C. Culture media was then added and the cells were incubated in hypoxia for 0, 0.5, and 1 hour. The cells were fixed in a mixture of 4% paraformaldehyde and 0.15 mol/l Na cacodylate buffer for 1 hour and postfixed in 0.5% OsO_4 in 0.1 mol/l Na cacodylate buffer for 1.5 hours at 8°C. The contrast was increased by incubation with 0.5% uranylacetate for 1 hour. Specimens were dehydrated by a progressive increase of ethanol concentration (70.0%–99.5% over 1 hour) and thereafter imbedded in agar 100 resin and allowed to polymerize for 70 hours. Ultrathin sections were obtained with a Reichert Ultracut E ultramicrotome (Leica Microsystems) and were collected on nickel grids. Sections were examined in a LEO 912AB Omega transmission electron microscope (Carl Zeiss NTS). Digital image files were captured with a MegaView III camera (Soft Imaging Systems).

Lipoprotein uptake. To investigate the effect of exogenous lipoproteins, HL-1 cells were incubated in media containing either standard serum or lipoprotein-deficient serum (Sigma-Aldrich) during the 8-hour hypoxic incubation period. Triglyceride-rich lipoproteins were isolated from mouse plasma as previously described (68) and labeled with 1,1′-dioctadecyl-1-3,3,3′,3′-tetramethylindocarbocyanin (Dil) (69). HL-1 cells in normoxia or hypoxia were incubated with 10 μg/ml of Dil-labeled triglyceride-rich lipoproteins for the final 3 hours of the 48-hour siRNA incubation. Micrographs were captured by confocal microscopy, and lipoprotein uptake was determined by measuring the intracellular fluorescent area of each cell as described previously (54).

LPL activity. Total LPL activity in HL-1 whole cell lysates was determined as described previously (70).

Measurement of TUNEL staining. TUNEL staining was performed in 8-μm slices of mouse hearts at the level of infarction using ApopTag ISOL Dual Fluorescence Apoptosis Detection Kit (Millipore) according to the manufacturer's instructions. The stained samples were analyzed by microscopy.

Lipid species analysis. Mouse hearts and human heart biopsies were homogenized in 70% methanol at 4°C for 5 minutes at 20 Hz. Known amounts of internal standards were added to the samples before extraction, and the final lipid extracts were dried under nitrogen. Sphingolipids and glycerolipids were extracted as described previously (56) and reconstituted in chloroform-methanol (1:2 vol/vol). Sphingolipids were analyzed as described in ref. 71 on a 4000 QTRAP mass spectrometer (Applied Biosystems/MDS Analytical Technologies) equipped with an ultra-high-pressure liquid chromatography (UHPLC) system, CTC PAL autosampler (Leap Technologies), and Rheos Allegro UHPLC (Flux Instruments) using multiple-reaction monitoring. Glycerolipids were analyzed by multiple precursor ion scanning as previously described (72) on a QTRAP 5500 mass spectrometer (Applied Biosystems/MDS Analytical Technologies) equipped with a robotic nanoflow ion source NanoMate HD (Advion). Mass spectrometry data files were processed using MultiQuant 1.1.0.26 or Lipid Profiler (73) (Applied Biosystems/MDS Analytical Technologies). Identified lipids were quantified by normalizing against their respective internal standard and tissue wet weight. Levels of acyl-CoA were analyzed as previously described (74).

Incubation of HL-1 cells with ceramide. HL-1 cells were incubated with 3.5 μmol/l ceramide (N-arachidoyl-D-*erythro*-sphingosine [C20 ceramide d18:1/20:0] and N-behenoyl-D-*erythro*-sphingosine [C22 ceramide d18:1/22:0] or N-lignoceroyl-D-*erythro*-sphingosine [C24 ceramide d18:1/24:0] and N-nervonoyl-D-*erythro*-sphingosine [C24:1 ceramide d18:1/24:1(15Z)]) (Avanti Polar Lipids) in ethanol/dodecane (98:2) (75) for 8 hours.

Echocardiography. Transthoracic echocardiography was performed on *Vldlr*$^{+/+}$ and *Vldlr*$^{-/-}$ mice at rest and during dobutamine stress (dobutamine 1 μg/g body weight was given intraperitoneally). During the procedure, the mice were maintained lightly anesthetized with an isoflurane dose of approximately 1.2% in air using a nose mask. Examinations were performed using a high-frequency 15-MHz linear transducer (CL 15-7; Philip Medical System) connected to an HDI 5000 ultrasound system (ATL; Philip Medical System). A warming pad was used to maintain normal body temperature. All data were stored and later evaluated offline on an Echo-Pac (Vingmed) system by one investigator blinded to the identity of the mice. For optimal orientation, the long-axis view was first performed and M-mode of left ventricular outflow tract (LVOT) measured. From an optimal parasternal short-axis view at the level of the papillary muscles, 2-dimensional targeted M-mode measurements of left ventricular internal diameters and wall thickness were obtained by using the leading-edge method of the American Society of Echocardiography. End diastole was defined as the largest left ventricular dimension and end systole as the peak inward motion of ventricular septum. All measurements were based on the average of at least 3 cardiac cycles. The following parameters were measured from short axis view: left ventricular diameter in diastole (LVEDd), left ventricular diameter in systole (LVEDs) and left ventricular posterior wall thickness (LVPWd). Fractional shortening was calculated as (LVEDd – LVESd) / LVEDd × 100. Two-dimensionally guided pulse Doppler recordings of left ventricular outflow were obtained from the apical "4-chamber" view for measurements of heart rate and aortic velocity time integral. Cardiac index was calculated as aorta velocity time integral × (π × (LVOT / 2)^2) / body weight and relative wall thickness as 2 × LVPWd / LVEDd. Doppler tissue imaging measurements were obtained for systolic and diastolic velocities from left ventricular posterior wall in the short-axis view. Because the groups were age matched and therefore differed in body weight, all measurements affected by size were divided by body weight. This protocol was approved by the Gothenburg Ethical Committee on Animal Experiments.

Statistics. Differences between groups were assessed using Mann-Whitney rank sum tests or 1-way ANOVA followed by the Dunette or Bonferroni post hoc test to determine statistical significance. Spearman's rank correlation was used to test the relationships between 2 variables. *P* values less than 0.05 were considered significant, and data are shown as mean ± SEM unless otherwise indicated.

Acknowledgments

We thank Rosie Perkins for very valuable and stimulating discussions and for editing the manuscript, Maria Heyden and Kristina SkÅlén for expert technical assistance, Azra Miljanovic for assistance in echocardiography measurements, Mikael Brisslert for help with FACS, and Bengt R. Johansson for help with electron microscopy experiments. This work was supported by the Swedish Research Council, the Swedish Heart-Lung Foundation, the Novo Nordisk Foundation, The Swedish Diabetes Society, Torsten, and Ragnar Söderberg Foundation, Swedish Foundation for Strategic Research, NIH grant HL054710, and the European Union–funded projects ETHERPATHS and Lipidomic Net.

Received for publication March 22, 2010, and accepted in revised form April 20, 2011.

Address correspondence to: Jan Borén, Wallenberg Laboratory, Sahlgrenska University Hospital, Bruna StrÅket 16, SE-413 45 Göteborg, Sweden. Phone: 46.31.342.2949; Fax: 46.31.823.762; E-mail: jan.boren@wlab.gu.se.

1. Bilheimer DW, Buja LM, Parkey RW, Bonte FJ,Willerson JT. Fatty acid accumulation and abnormal lipid deposition in peripheral and border zones of experimental myocardial infarcts. *J Nucl Med*. 1978;19(3):276–283.
2. Huss JM, Levy FH,Kelly DP. Hypoxia inhibits the peroxisome proliferator-activated receptor alpha/retinoid X receptor gene regulatory pathway in cardiac myocytes: a mechanism for O2-dependent modulation of mitochondrial fatty acid oxidation. *J Biol Chem*. 2001;276(29):27605–27612.
3. Hochachka PW, Buck LT, Doll CJ, Land SC. Unifying theory of hypoxia tolerance: molecular/metabolic defense and rescue mechanisms for surviving oxygen lack. *Proc Natl Acad Sci U S A*. 1996;93(18):9493–9498.
4. Abdel-Aleem S, St Louis JD, Hughes GC, Lowe JE. Metabolic changes in the normal and hypoxic neonatal myocardium. *Ann N Y Acad Sci*. 1999; 874:254–261.
5. Park TS, Yamashita H, Blaner WS, Goldberg IJ. Lipids in the heart: a source of fuel and a source of toxins. *Curr Opin Lipidol*. 2007;18(3):277–282.
6. Koonen DP, Glatz JF, Bonen A, Luiken JJ. Long-chain fatty acid uptake and FAT/CD36 translocation in heart and skeletal muscle. *Biochim Biophys Acta*. 2005;1736(3):163–180.
7. Unger RH. Lipotoxic diseases. *Annu Rev Med*. 2002; 53:319–336.
8. Schaffer JE. Lipotoxicity: when tissues overeat. *Curr Opin Lipidol*. 2003;14(3):281–287.
9. Slawik M, Vidal-Puig AJ. Lipotoxicity, overnutrition and energy metabolism in aging. *Ageing Res Rev*. 2006;5(2):144–164.
10. van Herpen NA, Schrauwen-Hinderling VB. Lipid accumulation in non-adipose tissue and lipotoxicity. *Physiol Behav*. 2008;94(2):231–241.
11. Olofsson SO, Bostrom P, Andersson L, Rutberg M, Perman J, Boren J. Lipid droplets as dynamic organelles connecting storage and efflux of lipids. *Biochim Biophys Acta*. 2009;1791(6):448–458.
12. Koliwad SK, et al. DGAT1-dependent triacylglycerol storage by macrophages protects mice from diet-induced insulin resistance and inflammation. *J Clin Invest*. 2010;120(3):756–767.
13. Rutkowski DT, Hegde RS. Regulation of basal cellular physiology by the homeostatic unfolded protein response. *J Cell Biol*. 2010;189(5):783–794.
14. Hegde RS, Ploegh HL. Quality and quantity control at the endoplasmic reticulum. *Curr Opin Cell Biol*. 2010;22(4):437–446.
15. Minamino T, Komuro I, Kitakaze M. Endoplasmic reticulum stress as a therapeutic target in cardiovascular disease. *Circ Res*. 2010;107(9):1071–1082.
16. Chabowski A, Gorski J, Calles-Escandon J, Tandon NN, Bonen A. Hypoxia-induced fatty acid transporter translocation increases fatty acid transport and contributes to lipid accumulation in the heart. *FEBS Lett*. 2006;580(15):3617–3623.
17. Chun YS, et al. Hypoxic activation of the atrial natriuretic peptide gene promoter through direct and indirect actions of hypoxia-inducible factor-1. *Biochem J*. 2003;370(pt 1):149–157.
18. Tacken PJ, Hofker MH, Havekes LM, van Dijk KW. Living up to a name: the role of the VLDL receptor in lipid metabolism. *Curr Opin Lipidol*. 2001;12(3):275–279.
19. Takahashi S, Sakai J, Fujino T, Miyamori I, Yamamoto TT. The very low density lipoprotein (VLDL) receptor--a peripheral lipoprotein receptor for remnant lipoproteins into fatty acid active tissues. *Mol Cell Biochem*. 2003;248(1–2):121–127.
20. Yagyu H, et al. Very low density lipoprotein (VLDL) receptor-deficient mice have reduced lipoprotein lipase activity. Possible causes of hypertriglyceridemia and reduced body mass with VLDL receptor deficiency. *J Biol Chem*. 2002;277(12):10037–10043.
21. Goudriaan JR, et al. The VLDL receptor plays a major role in chylomicron metabolism by enhancing LPL-mediated triglyceride hydrolysis. *J Lipid Res*. 2004;45(8):1475–1481.
22. Burke JF Jr, et al. Long-term efficacy and safety of cyclosporine in renal-transplant recipients. *N Engl J Med*. 1994;331(6):358–363.
23. Kitakaze M, Tsukamoto O. What is the role of ER stress in the heart? Introduction and series overview. *Circ Res*. 2010;107(1):15–18.
24. Menuz V, et al. Protection of C. elegans from anoxia by HYL-2 ceramide synthase. *Science*. 2009; 324(5925):381–384.
25. Yang J, et al. CD36 deficiency rescues lipotoxic cardiomyopathy. *Circ Res*. 2007;100(8):1208–1217.
26. Finck BN, et al. The cardiac phenotype induced by PPARalpha overexpression mimics that caused by diabetes mellitus. *J Clin Invest*. 2002;109(1):121–130.
27. Loewen N, Chen J, Dudley VJ, Sarthy VP, Mathura JR Jr. Genomic response of hypoxic Muller cells involves the very low density lipoprotein receptor as part of an angiogenic network. *Exp Eye Res*. 2009;88(5):928–937.
28. Nakazato K, et al. Expression of very low density lipoprotein receptor mRNA in circulating human monocytes: its up-regulation by hypoxia. *Atherosclerosis*. 2001;155(2):439–444.
29. Duncan JG, et al. Rescue of cardiomyopathy in peroxisome proliferator-activated receptor-alpha transgenic mice by deletion of lipoprotein lipase identifies sources of cardiac lipids and peroxisome proliferator-activated receptor-alpha activators. *Circulation*. 2010;121(3):426–435.
30. Bosch X, Theroux P. Left ventricular ejection fraction to predict early mortality in patients with non-ST-segment elevation acute coronary syndromes. *Am Heart J*. 2005;150(2):215–220.
31. Bradshaw PJ, Ko DT, Newman AM, Donovan LR, Tu JV. Validation of the Thrombolysis In Myocardial Infarction (TIMI) risk index for predicting early mortality in a population-based cohort of STEMI and non-STEMI patients. *Can J Cardiol*. 2007;23(1):51–56.
32. Lopaschuk GD. Metabolic abnormalities in the diabetic heart. *Heart Fail Rev*. 2002;7(2):149–159.
33. Mathieu P, Pibarot P, Larose E, Poirier P, Marette A, Despres JP. Visceral obesity and the heart. *Int J Biochem Cell Biol*. 2008;40(5):821–836.
34. Rijzewijk LJ, et al. Myocardial steatosis is an independent predictor of diastolic dysfunction in type 2 diabetes mellitus. *J Am Coll Cardiol*. 2008;52(22):1793–1799.
35. Ng AC, et al. Myocardial steatosis and biventricular strain and strain rate imaging in patients with type 2 diabetes mellitus. *Circulation*. 2010; 122(24):2538–2544.
36. Adiels M, Olofsson SO, Taskinen MR, Boren J. Overproduction of very low-density lipoproteins is the hallmark of the dyslipidemia in the metabolic syndrome. *Arterioscler Thromb Vasc Biol*. 2008;28(7):1225–1236.
37. Junttila MJ, et al. Sudden cardiac death after myocardial infarction in patients with type 2 diabetes. *Heart Rhythm*. 2010;7(10):1396–1403.
38. Ferre P, Foufelle F. Hepatic steatosis: a role for de novo lipogenesis and the transcription factor SREBP-1c. *Diabetes Obes Metab*. 2010;12 suppl 2:83–92.
39. Flamment M, Kammoun HL, Hainault I, Ferre P, Foufelle F. Endoplasmic reticulum stress: a new actor in the development of hepatic steatosis. *Curr Opin Lipidol*. 2010;21(3):239–246.
40. Pineau L, Ferreira T. Lipid-induced ER stress in yeast and beta cells: parallel trails to a common fate. *FEMS Yeast Res*. 2010;10(8):1035–1045.
41. Schenck M, Carpinteiro A, Grassme H, Lang F, Gulbins E. Ceramide: physiological and pathophysiological aspects. *Arch Biochem Biophys*. 2007;462(2):171–175.
42. Noureddine L, et al. Modulation of total ceramide and constituent ceramide species in the acutely and chronically hypoxic mouse heart at different ages. *Prostaglandins Other Lipid Mediat*. 2008;86(1–4):49–55.
43. Crowder CM. Cell biology. Ceramides--friend or foe in hypoxia? *Science*. 2009;324(5925):343–344.
44. Hotamisligil GS. Endoplasmic reticulum stress and the inflammatory basis of metabolic disease. *Cell*. 2010;140(6):900–917.
45. Selye H, Bajusz E, Grasso S, Mendell P. Simple techniques for the surgical occlusion of coronary vessels in the rat. *Angiology*. 1960;11:398–407.
46. Abbate A, et al. Anakinra, a recombinant human interleukin-1 receptor antagonist, inhibits apoptosis in experimental acute myocardial infarction. *Circulation*. 2008;117(20):2670–2683.
47. Ruiz J, et al. The apoE isoform binding properties of the VLDL receptor reveal marked differences from LRP and the LDL receptor. *J Lipid Res*. 2005;46(8):1721–1731.
48. Ananyeva NM, et al. The binding sites for the very low density lipoprotein receptor and low-density lipoprotein receptor-related protein are shared within coagulation factor VIII. *Blood Coagul Fibrinolysis*. 2008;19(2):166–177.
49. Karason K, Jernas M, Hagg DA, Svensson PA. Evaluation of CXCL9 and CXCL10 as circulating biomarkers of human cardiac allograft rejection. *BMC Cardiovasc Disord*. 2006;6:29.
50. Claycomb WC, et al. HL-1 cells: a cardiac muscle cell line that contracts and retains phenotypic characteristics of the adult cardiomyocyte. *Proc Natl Acad Sci U S A*. 1998;95(6):2979–2984.
51. Nicholson DW, et al. Identification and inhibition of the ICE/CED-3 protease necessary for mammalian apoptosis. *Nature*. 1995;376(6535):37–43.
52. Nicoletti A, Kaveri S, Caligiuri G, Bariety J, Hansson GK. Immunoglobulin treatment reduces atherosclerosis in apo E knockout mice. *J Clin Invest*. 1998;102(5):910–918.
53. Bostrom P, et al. Cytosolic lipid droplets increase in size by microtubule-dependent complex formation. *Arterioscler Thromb Vasc Biol*. 2005;25(9):1945–1951.
54. Bostrom P, et al. Hypoxia converts human macrophages into triglyceride-loaded foam cells. *Arterioscler Thromb Vasc Biol*. 2006;26(8):1871–1876.
55. Magnusson B, et al. Adipocyte differentiation-related protein promotes fatty acid storage in cytosolic triglycerides and inhibits secretion of very low-density lipoproteins. *Arterioscler Thromb Vasc Biol*. 2006;26(7):1566–1571.
56. Ekroos K, Chernushevich IV, Simons K, Shevchenko A. Quantitative profiling of phospholipids by multiple precursor ion scanning on a hybrid quadrupole time-of-flight mass spectrometer. *Anal Chem*. 2002;74(5):941–949.
57. Homan R, Anderson MK. Rapid separation and quantitation of combined neutral and polar lipid classes by high-performance liquid chromatography and evaporative light-scattering mass detection. *J Chromatogr B Biomed Sci Appl*. 1998;708(1–2):21–26.
58. Perfetto SP, Chattopadhyay PK, Roederer M. Seventeen-colour flow cytometry: unravelling the immune system. *Nat Rev Immunol*. 2004;4(8):648–655.
59. Hansson PK, Asztely AK, Clapham JC, Schreyer SA. Glucose and fatty acid metabolism in McA-RH7777 hepatoma cells vs. rat primary hepatocytes: responsiveness to nutrient availability. *Biochim Biophys Acta*. 2004;1684(1–3):54–62.
60. Olefsky JM. Mechanisms of the ability of insulin to activate the glucose-transport system in rat adipocytes. *Biochem J*. 1978;172(1):137–145.
61. Bostrom P, et al. SNARE proteins mediate fusion between cytosolic lipid droplets and are implicated in insulin sensitivity. *Nat Cell Biol*. 2007; 9(11):1286–1293.
62. Andersson L, et al. PLD1 and ERK2 regulate cytosolic lipid droplet formation. *J Cell Sci*. 2006;119(pt 11):2246–2257.
63. Hoe HS, Rebeck GW. Regulation of ApoE receptor

proteolysis by ligand binding. *Brain Res Mol Brain Res*. 2005;137(1–2):31–39.
64. Henry RR, Abrams L, Nikoulina S, Ciaraldi TP. Insulin action and glucose metabolism in nondiabetic control and NIDDM subjects. Comparison using human skeletal muscle cell cultures. *Diabetes*. 1995;44(8):936–946.
65. Klip A, Logan WJ, Li G. Hexose transport in L6 muscle cells. Kinetic properties and the number of [3H]cytochalasin B binding sites. *Biochim Biophys Acta*. 1982;687(2):265–280.
66. Rydberg EK, et al. Hypoxia increases 25-hydroxycholesterol-induced interleukin-8 protein secretion in human macrophages. *Atherosclerosis*. 2003;170(2):245–252.
67. Takazawa T, et al. Peroxisome proliferator-activated receptor gamma agonist rosiglitazone increases expression of very low density lipoprotein receptor gene in adipocytes. *J Biol Chem*. 2009;284(44):30049–30057.
68. Olofsson SO, Bostrom K, Svanberg U, Bondjers G. Isolation and partial characterization of a polypeptide belonging to apolipoprotein B from low-density lipoproteins of human plasma. *Biochemistry*. 1980;19(6):1059–1064.
69. Innerarity TL, Pitas RE, Mahley RW. Lipoprotein-receptor interactions. *Methods Enzymol*. 1986;129:542–565.
70. Gustafsson M, et al. Retention of low-density lipoprotein in atherosclerotic lesions of the mouse: evidence for a role of lipoprotein lipase. *Circ Res*. 2007;101(8):777–783.
71. Merrill AH Jr, Sullards MC, Allegood JC, Kelly S, Wang E. Sphingolipidomics: high-throughput, structure-specific, and quantitative analysis of sphingolipids by liquid chromatography tandem mass spectrometry. *Methods*. 2005;36(2):207–224.
72. Stahlman M, Ejsing CS, Tarasov K, Perman J, Boren J, Ekroos K. High-throughput shotgun lipidomics by quadrupole time-of-flight mass spectrometry. *J Chromatogr B Analyt Technol Biomed Life Sci*. 2009;877(26):2664–2672.
73. Ejsing CS, et al. Automated identification and quantification of glycerophospholipid molecular species by multiple precursor ion scanning. *Anal Chem*. 2006;78(17):6202–6214.
74. Haynes CA, Allegood JC, Sims K, Wang EW, Sullards MC, Merrill AH Jr. Quantitation of fatty acyl-coenzyme As in mammalian cells by liquid chromatography-electrospray ionization tandem mass spectrometry. *J Lipid Res*. 2008;49(5):1113–1125.
75. Hartfield PJ, Mayne GC, Murray AW. Ceramide induces apoptosis in PC12 cells. *FEBS Lett*. 1997;401(2–3):148–152.